J. Appl. Comput. Mech., 9(2) (2023) 529-549
DOI: 10.22055/jacm.2022.41537.3770

ISSN: 2383-4536
jacm.scu.ac.ir

Shahid Chamran University of Ahvaz

Journal of Applied and Computational Mechanics

Research Paper

A Systematic Computational and Experimental Study of the Principal Data-Driven Identification Procedures. Part I: Analytical Methods and Computational Algorithms

Carmine Maria Pappalardo[1], Filippo Califano[2], Sefika Ipek Lok[3], Domenico Guida[4]

[1]Department of Industrial Engineering, University of Salerno, Via Giovanni Paolo II, 132, Fisciano, 84084, Salerno, Italy, Email: cpappalardo@unisa.it
[2]Spin-Off MEID4 s.r.l., University of Salerno, Via Giovanni Paolo II, 132, Fisciano, 84084, Salerno, Italy, Email: i.f.califano@gmail.com
[3]Department of Mechatronics Engineering, The Graduate School of Natural and Applied Sciences, Dokuz Eylul University, Turkiye, Email: sefikaipeklok@gmail.com
[4]Department of Industrial Engineering, University of Salerno, Via Giovanni Paolo II, 132, Fisciano, 84084, Salerno, Italy, Email: guida@unisa.it

Received August 3 2022; Revised October 29 2022; Accepted for publication November 12 2022.
Corresponding author: Carmine Maria Pappalardo (cpappalardo@unisa.it)

Abstract. This paper is the first part of a two-part research work aimed at performing a systematic computational and experimental analysis of the principal data-driven identification procedures based on the Observer/Kalman Filter Identification Methods (OKID) and the Numerical Algorithms for Subspace State-Space System Identification (N4SID). Considering the approach proposed in this work, the state-space model of a mechanical system can be identified with the OKID and N4SID methods. Additionally, the second-order configuration-space dynamical model of the mechanical system of interest can be estimated with the MKR (Mass, Stiffness, and Damping matrices) and PDC (Proportional Damping Coefficients) techniques. In particular, this first paper concentrates on the description of the fundamental analytical methods and computational algorithms employed in this study. In this investigation, numerical and experimental analyses of two fundamental time-domain system identification techniques are performed. To this end, the main variants of the OKID and the N4SID methods are examined in this study. These two families of numerical methods allow for identifying a first-order state-space model of a given dynamical system by directly starting from the time-domain experimental data measured in input and output to the system of interest. The basic steps of the system identification numerical procedures mentioned before are described in detail in the paper. As discussed in the manuscript, from the identified first-order state-space dynamical models obtained using the OKID and N4SID methods, a second-order configuration-space mechanical model of the dynamic system under consideration can be subsequently obtained by employing another identification algorithm described in this work and referred to as the MKR method. Furthermore, by using the second-order dynamical model obtained from experimental data, and considering the hypothesis of proportional damping, an effective technique referred to as the PDC method is also introduced in this investigation to calculate an improved estimation of the identified damping coefficients. In this investigation, a numerical and experimental comparison between the OKID methods and the N4SID algorithms is proposed. Both families of methodologies allow for performing the time-domain state-space system identification, namely, they lead to an estimation of the state, input influence, output influence, and direct transmission matrices that define the dynamic behavior of a mechanical system. Additionally, a least-square approach based on the PDC method is employed in this work for reconstructing an improved estimation of the damping matrix starting from a triplet of estimated mass, stiffness, and damping matrices of a linear dynamical system obtained using the MKR identification procedure. The mathematical background thoroughly analyzed in this first research work serves to pave the way for the applications presented and discussed in the second research paper.

Keywords: Applied System Identification, Experimental Modal Analysis, Observer/Kalman Filter Identification Methods (OKID), Numerical Algorithms for Subspace State-Space System Identification (N4SID), Mass, Stiffness, and Damping Matrices Identification (MKR).

1. Introduction

In this section, an overview of the problems addressed in the first part of this two-part paper is reported. For this purpose, this introduction section covers several important topics, such as some fundamental background material on the computational and experimental methods of applied system identification, a literature review describing the principal developments that can be found in the field of reference focused on system identification and vibration control, a summary of the contributions within the scope of the present work, and the structure used to organize this manuscript.

1.1 Background Material and Research Significance

From a wide perspective, system identification can be defined as the iterative process aimed at developing or improving the mathematical model of a given physical system using experimental observations [1]. This versatile computational technique is based on the input and output data available, which are typically obtained in the presence of disturbances and/or noise [2]. Therefore, all system identification methods are based on input and output signals, recorded from the system to be identified, and have the main goal of constructing the most accurate and robust mathematical model that fits the observed data [3,4]. In general, an identified model should be accurate in the sense that it must reproduce the dynamic behavior of the system of interest, namely a numerical set of output data that is identical to the original set of output measurements recorded on the real system in correspondence with the same set of input excitations [5]. Furthermore, an identified mathematical model is said to be robust when it is able to reproduce, to a certain degree, the same output measurements obtained from the real system to be identified, even when the excitation signals have a frequency content that is distant from the one used to perform the identification process [6,7]. Thus, the development of system identification techniques that lead to accurate and robust mathematical models represents a challenging task that can be properly exploited in several engineering applications [8,9].

This paper is part of a wider framework in which the research of the authors is collocated. The research outline of the authors is concerned with the inter-dependencies between three main fields of interest that are multibody system dynamics, nonlinear optimal control, and applied system identification. Multibody system dynamics deals with the dynamic analysis of mechanical systems constrained by kinematic joints and subjected to external forces as well as driving control actions [10–12]. Nonlinear optimal control is the scientific discipline that studies the advanced methods suitable for the design of effective control laws which can be successfully implemented in the case of nonlinear dynamical systems [13,14]. Applied system identification can be defined as the art of creating linear and/or nonlinear mathematical models of physical systems using experimental data and resorting to the basic principles of mechanics [15,16]. Therefore, the present research work fits the third field of research of the authors. This investigation is indeed focused on performing a comparative analysis of the two principal data-driven identification procedures of interest for practical engineering applications. The computational procedures considered in this work are based on the numerical methods of dynamic identification developed in the domain of time.

As discussed in detail below, immediately after a detailed literature survey on the issues of interest for this work, the central problem that represents the object of this investigation is the definition and the comparison of appropriate numerical procedures based on input-output experimental signals to construct first-order state-space dynamical models and/or second-order configuration-space dynamical models of linear time-invariant mechanical systems.

1.2 Literature Review on System Identification and Vibration Control

The system identification approach was firstly developed for control theory applications [17]. However, in the last twenty years, the system identification approach has become an independent field of scientific research that is used to estimate mathematical models of physical systems and describe the kinematic and dynamic behaviors of mechanical systems using simulation or experimental data [2]. In the literature, state-space system identification methods, such as the combination of the Observer/Kalman Filter Identification Method (OKID) with the Eigensystem Realization Algorithm (ERA) and the Numerical Algorithms for Subspace State-Space System Identification (N4SID), are effectively used to describe mechanical systems [1,3]. Valasek et al. applied the OKID method to a six-degree-of-freedom simulation of an AV-8B Harrier for online identification [18]. Tiano et al. studied experimental identification of an autonomous underwater vehicle [19]. Heredia et al. studied sensor fault detection of unmanned aerial vehicles with the OKID method using real helicopter flight data [20]. Yang et al. presented a structural damage identification method applied to a five-story linear shear-beam type building employing the extended Kalman filter approach and using vibration signals [21]. Abreu et al. studied the vibration modeling and control of a flexible aluminum beam using the OKID method together with the ERA method [22]. Gagg Filho et al. studied the experimental identification of a cantilever beam, which was driven with white noise, and a linear quadratic regulator method was applied to the estimated model for determining the first two natural frequencies of the system of interest [23]. Ni et al. modeled a flexible space manipulator to identify its payload parameters, such as the mass and the moments of inertia, using torque input and vibration signals [24]. In [25], Favoreel et al. compared the results of a prediction error method applied to industrial processes and the performance of several subspace identification techniques, such as the N4SID, the IV-4SID, the Multivariable Output-Error State sPace (MOESP), and the Canonical Variate Analysis (CVA) procedures. In [26], Douat et al. modeled a parallel robot and achieved the vibration attenuation of its endpoint with two degrees of freedom using the N4SID family of identification methods. In [27], Costa Junior et al. applied the subspace identification method together with the N4SID technique to a robotic manipulator with five degrees of freedom. In [28], Costa Junior et al. estimated a discrete-time linear state-space model of a prototype of a jaw crusher using the N4SID method with appropriate MOESP weighting matrices. In [29], a methodology was proposed for deriving physical parameters from the state-space models of mechanical systems. De Angelis et al. developed a new solution for the identification of physical parameters of mechanical systems from dynamical models identified in the state space [30]. While a full set of sensors and a full set of actuators were needed to obtain the physical parameters in their previous research work, Angeles et al. proposed in [31,32] a new approach that requires only one sensor or one actuator at all degrees of freedom. Rabah et al. applied the N4SID identification algorithms to a sewage sludge incineration process [33]. Anandakumar et al. identified the structural and crack parameters in a continuous mass model using the OKID and ERA techniques [34]. In [35], Piramoon et al. used the OKID and ERA identification techniques to identify the modal parameters of a centrifugal machine. Iyer et al. identified the modal parameters of a coaxial octocopter using the ERA-OKID algorithm [36]. In [37], Huang et al. revised the kinematics, dynamics, and optimization of parallel robots with lower mobility.

In [38], Phan et al. analyzed a time-domain method for identifying a state-space model of a linear system given a general set of input-output data. Guida et al. analyzed and tested the ERA-OKID identification method on a linear mechanical system [39]. In [40], Sampaio Silveira Júnior et al. automatically estimated the parameters of the fuzzy model through multivariable input and output data sets using proper identification methodologies such as OKID and ERA methods. Subramanian et al. implemented several identification algorithms for a four tank system demonstrating the superiority of the N4SID method [41]. Manrique-Escobar et al. analyzed the main aspects concerning the kinematic, dynamic, control, and identification characteristics of two-wheeled vehicles modeled as articulated mechanical systems using the multibody formulation approach [42]. In [43], Pappalardo and Guida analyzed and tested the ERA-OKID algorithm to identify a second-order mechanical model related to the structure of interest. They also developed and tested a method to reduce the vibrations induced on structural systems based on new inertial-based vibration absorber [44]. Borjas et al. focused on implementing N4SID and MOESP identification techniques for industrial processes [45]. In [46], Juricek et al. discussed and tested various system identification numerical techniques such as, in particular, the CVA and the N4SID procedures. In [47], Mola et al. developed a new identification method using the Local Linear Model Trees (LOLIMOT) toolbox for nonlinear system identification implemented in MATLAB and subsequently tested their approach on a flexible robot arm. In [48], Brunton et al. investigated the identification and feedback control of unstable and imprecise dynamic models. Tronci et al. studied the vibration analysis of the Rieti civic tower using the OKID identification algorithm and tried to determine the integrity level of the structure [49]. Borjas et al. tested the ERA-OKID identification algorithms in the presence of slight nonlinearities [50]. In [51], Mercère et al. studied the problem of identifying multiple models in the presence of several inputs and outputs. Deistler et al. provided a coherence test between two subspatial methods through a simulation study [52]. Peternell et al. introduced three new dynamic identification algorithms and compared them with the identification obtained through the N4SID algorithm [53]. In

[54], Jamaludin et al. analyzed the MOESP and N4SID algorithms. Flint et al. described a statistical performance analysis method for subspatial systems identification algorithms [55]. In [56], Simay et al. compared the different identification algorithms of the subspatial procedures referred to as N4SID, CVA, and MOESP. Heredia et al. presented a small autonomous helicopter failure detection and diagnosis system using a sensor and the OKID identification algorithm [57]. In [58], Chang et al. focused on improving the OKID algorithm by providing experimental data and a comparison with other identification algorithms. In [59], Qin provided an overview of subspatial identification methods for open-loop and closed-loop systems. Dong et al. studied the efficiency of the OKID identification algorithm with numerical simulations and experimental studies of active vibration control [60]. In [61], Wang et al. presented a variant of the OKID algorithm for the identification of unknown nonlinear dynamic systems. Bauer et al. examined the asymptotic properties of the MOESP algorithm [62]. In [63, 64], the dynamic analysis of a large deployable reflector and its opening system was performed and an optimized geometry was found by measuring the error around the feed.

Aktas et al. carried out the experimental modal analysis on a large number of samples to investigate the damping characteristics of sleepers for railways applications [65]. Wang et al. proposed a camera-based experimental modal analysis with impact excitation considering an experimental validation on a clamped-clamped beam excited by an impact hammer [66]. Koyuncu et al. determined a mathematical model of an amplified stack-type piezoelectric actuator employing a nonlinear system identification method for performing the experimental modal analysis [67]. Song et al. proposed a numerical and experimental method to predict the modal properties of the three-dimensional multi-axial hybrid composite materials for engineering applications [68]. Berninger et al. studied the effects of structural dynamics on the performance of biped walking robots by using the applied methods for the experimental modal analysis [69]. The computational methods of applied system identification are also used to improve the mathematical model of lithium-ion batteries by considering the time variations in the current, voltage, and temperature [70, 71]. To this end, Wang et al. carried out an experimental study considering system identification methods of fractional-order mathematical models aimed at describing lithium-ion batteries and ultra-capacitors [72]. In [73], Peng et al. analyzed the State of charge (SOC) of lithium-ion batteries and used an improved Adaptive Dual Unscented Kalman Filter (ADUKF) method to estimate the unknown parameters of the battery mathematical model. In [74], Ren et al. proposed an improved recursive least square algorithm for the parameter identification of the mathematical model of a lithium-ion battery. The large number of scientific works found in the literature demonstrates the importance and the interconnections between the complex fields of research concerning structural dynamics, system identification, and optimal control.

1.3 Scope and Contributions of this Study

This paper is the first part of a two-part research work intended at performing a systematic computational and experimental analysis of the principal data-driven identification procedures based on the Observer/Kalman Filter Identification Methods (OKID) and the Numerical Algorithms for Subspace State-Space System Identification (N4SID). More specifically, this first paper focuses on the description of the fundamental analytical methods and computational algorithms employed in this investigation.

The system identification methodologies of interest for this research work are the OKID method (Observer/Kalman Filter Identification Methods) and the N4SID algorithm (Numerical Algorithms for Subspace State-Space System Identification). In this paper, the fundamental aspects that stand behind the computer implementation of the numerical and experimental comparisons of the two fundamental system identification techniques mentioned before are thoroughly analyzed. Both the OKID and the N4SID numerical procedures can be effectively employed for identifying a first-order dynamical model of a mechanical system as well as to carry out the modal analysis of a structural system based on experimental measurements. More specifically, in this first paper, the mathematical background and the algorithmic steps of the principal variants inherent in the OKID procedure and the N4SID procedure are described, namely, the ERA-OKID method (Eigensystem Realization Algorithm), the ERA/DC-OKID method (Eigensystem Realization Algorithm with Data Correlation), the CVA-N4SID method (Canonical Variate Analysis), the MOESP-N4SID method (Multivariable Output-Error State sPace), and the SSARX-N4SID method (Subspace State-space AutoRegressive with eXogenous variables) are analyzed in detail.

This work is grounded in the field of the computational methods of applied system identification that are used for estimating the modal parameters of structural and mechanical systems. In particular, this investigation focuses on the development of a systematic comparison of the principal system identification numerical procedures that are based on time-domain data, which can be effectively used for obtaining time-invariant dynamical models of mechanical systems having a linear structure. For a general mechanical system, the state-space model identified by means of the numerical algorithms discussed in this work can be used for describing the system input-output mapping, as well as for computing the system natural frequencies, damping ratios, and mode shapes. In the second part of this research work, the effectiveness and efficiency of the identification methods considered in this investigation are tested through numerical experiments and by considering input-output experimental data obtained from a laboratory test rig. On the other hand, the first part of this research work focuses on the mathematical background and on the computational aspects of the main identification methods of interest for this investigation. To this end, this paper also focuses on the description of a method labeled as the MKR method that is suitable for extracting a second-order configuration-space model of a given mechanical system whose first-order state-space dynamical model was previously identified with the use of another identification algorithm, which is chosen, for example, between the OKID method and the N4SID technique. Finally, considering the hypothesis of proportional damping, which is always reasonable in the case of metallic structures having small internal dissipation effects, this paper reports a computational procedure called the PDC method for improving the estimation of the damping matrix of a mechanical system.

This investigation deals with the estimation of the structural parameters of mechanical systems using the computational methods of applied system identification. More specifically, this first paper is focused on the mathematical background necessary for obtaining first-order and second-order models of linear mechanical systems. The OKID and N4SID methods considered in this first paper are particularly suitable for this task since they allow for constructing an estimation of the state-space model of the dynamical system of interest using a proper set of input-output measurements. Additionally, the MKR method represents an effective technique for extracting a configuration-space model from an identified state-space model converted from the discrete-time domain to the continuous-time domain. The PDC procedure, on the other hand, is a viable tool for improving the estimation of the damping coefficients of a given mechanical system. The key points of these important identification procedures are described in detail in this paper to allow the reproduction of the results proposed in this work by other independent researchers interested in the topics analyzed in this investigation. Therefore, compared to the existing approaches, this first paper belonging to the present two-part research work proposes a systematic approach for identifying and refining the estimation of the structural parameters of mechanical systems when the focus is on experimental modal analysis.

A flowchart that conceptually describes the proposed approach is shown in Figure 1.

In summary, the proposed approach consists of four fundamental steps. In the first step, the experimental or numerical input and output signals of the structural system of interest are generated or measured. In the second step, the identification techniques are applied to estimate the mathematical models of the system under study using two different system identification methods, such as the OKID and N4SID methods. In the third step, the mass, spring, and damping matrices of the system of interest are determined

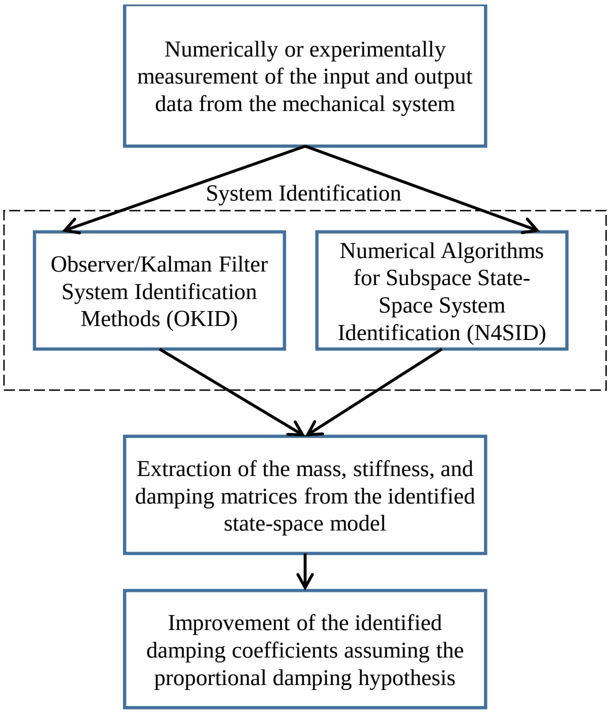

Fig. 1. *Flowchart of the proposed approach.*

by using the state space model estimated employing the MKR method. Since the damping matrix obtained by using the MKR method is negatively affected by the noise produced by the measurement apparatus, the PCD method is used in the fourth and last step to improve the estimation of the system damping.

Future research works will be devoted to the investigation of the performance of the ERA/OKID and N4SID families of identification procedures in the case of more complex mechanical systems such as, for example, three-dimensional vibrating systems in which the torsional natural frequencies are in the same range of the natural frequencies associated with the structural bending along two orthogonal directions.

1.4 Organization of the Manuscript

The remaining parts of this two-part manuscript are organized as follows. In Section 2., the basic analytical tools used to describe the dynamical behavior of mechanical systems characterized by a linear mathematical structure are recalled. Section 3. provides the fundamental algorithmic steps of the principal time-domain data-driven numerical procedures suitable for identifying state-space and configuration-space dynamical models of linear mechanical systems, as well as an operative method for improving the estimation of the damping matrix of a dynamical system. In Section 4., a summary of the manuscript, the conclusions reached in this two-part investigation, and some ideas for future research directions are given.

2. Linear Models of Dynamical Systems

In this section, the basic aspects necessary for defining linear dynamical models of structural systems are described. To this end, the transformation from the space of the configurations to the space of the states is introduced first. Subsequently, the substantial differences between continuous-time dynamical models and discrete-time dynamical models are highlighted. The latter family of state-space models directly arises from the former type of dynamical models and represents the fundamental starting point for the construction of the system identification numerical procedures useful in practical engineering applications. Finally, a sequence of discrete dynamical parameters grouped in a matrix form that is referred to as the set of Markov parameters is introduced.

2.1 Continuous-Time State-Space Dynamical Models

In this subsection, the general form of the dynamical model of a linear mechanical system is described considering the state-space representation in the continuous-time domain [2,75]. For this purpose, consider a mechanical system having a linear structure and endowed with n_f degrees of freedom. By using a coordinate representation based on a minimal set of generalized coordinates, the equations of motion for the linear dynamical system are mathematically represented by a set of $n_x = n_f$ linear differential equations of the second order having constant coefficients, where n_x is indeed the number of generalized coordinates that is equal to the degrees of freedom of the system. Thus, the equations of motion can be expressed using the following compact matrix notation:

$$\boldsymbol{M}\ddot{\boldsymbol{x}} + \boldsymbol{R}\dot{\boldsymbol{x}} + \boldsymbol{K}\boldsymbol{x} = \boldsymbol{F} \tag{1}$$

where $\boldsymbol{x} = \boldsymbol{x}(t)$, $\dot{\boldsymbol{x}} = d\boldsymbol{x}/dt$, and $\ddot{\boldsymbol{x}} = d\dot{\boldsymbol{x}}/dt = d^2\boldsymbol{x}/dt^2$ respectively represent the system generalized coordinate, velocity, and acceleration vectors having dimensions $n_x \times 1$, t is the time variable, while $\boldsymbol{K}$, $\boldsymbol{R}$, and $\boldsymbol{M}$ respectively identify the system stiffness, damping, and mass matrices having dimensions $n_x \times n_x$, whereas $\boldsymbol{F} = \boldsymbol{F}(t)$ embodies the system generalized external force vector having dimensions $n_x \times 1$. The generalized external force vector $\boldsymbol{F}$ can be conveniently rewritten in terms of an input vector $\boldsymbol{u} = \boldsymbol{u}(t)$ having dimensions $n_u \times 1$ by using an appropriate actuator collocation matrix denoted with $\boldsymbol{B}_a$ of dimensions $n_x \times n_u$ as follows:

$$\boldsymbol{F} = \boldsymbol{B}_a\boldsymbol{u} \tag{2}$$

where n_u represents the number of control inputs. The use of the generalized coordinate vector $\boldsymbol{x}$ allows for writing the system equations of motion in the configuration space. On the other hand, let's introducing the following state vector denoted with $\boldsymbol{z} = \boldsymbol{z}(t)$ and having dimensions $n_z \times 1$ with $n_z = 2n_x$:

$$\boldsymbol{z} = \begin{bmatrix} \boldsymbol{z}_1 \\ \boldsymbol{z}_2 \end{bmatrix} = \begin{bmatrix} \boldsymbol{x} \\ \dot{\boldsymbol{x}} \end{bmatrix} \tag{3}$$

By doing so, one can easily transform the previous configuration-space dynamic model into the following state-space dynamic model by adding an identity equation:

$$\begin{cases} \dot{\boldsymbol{z}}_1 = \boldsymbol{z}_2 \\ \dot{\boldsymbol{z}}_2 = -\boldsymbol{M}^{-1}\boldsymbol{K}\boldsymbol{z}_1 - \boldsymbol{M}^{-1}\boldsymbol{R}\boldsymbol{z}_2 + \boldsymbol{M}^{-1}\boldsymbol{B}_a\boldsymbol{u} \end{cases} \tag{4}$$

which can be written in the following compact matrix form:

$$\dot{\boldsymbol{z}} = \boldsymbol{A}_c\boldsymbol{z} + \boldsymbol{B}_c\boldsymbol{u} \tag{5}$$

where $\boldsymbol{A}_c$ represents the continuous-time system state matrix having dimensions $n_z \times n_z$ and $\boldsymbol{B}_c$ identifies the continuous-time input influence matrix of dimensions $n_z \times n_u$ which are respectively defined as:

$$\boldsymbol{A}_c = \begin{bmatrix} \boldsymbol{O} & \boldsymbol{I} \\ -\boldsymbol{M}^{-1}\boldsymbol{K} & -\boldsymbol{M}^{-1}\boldsymbol{R} \end{bmatrix}, \quad \boldsymbol{B}_c = \begin{bmatrix} \boldsymbol{O} \\ \boldsymbol{M}^{-1}\boldsymbol{B}_a \end{bmatrix} \tag{6}$$

In practical applications, one cannot directly measure the entire system state vector $\boldsymbol{z}$. Therefore, the system state must be reconstructed from a set of available measurements contained in an output vector denoted with $\boldsymbol{y} = \boldsymbol{y}(t)$ having dimensions $n_y \times 1$. In general, the dimension of the output vector n_y is smaller than the dimension of the state vector n_z. The output vector can be written as a linear combination of the system generalized displacements, velocities, and accelerations in relation to the particular types of sensors that are actually available in the experimental test rig. Thus, in order to mathematically model the sensor measurements, a set of measurement equations is added to the system continuous-time dynamic model. In the configuration space, the output equations can be readily expressed as follows:

$$\boldsymbol{y} = \boldsymbol{C}_p\boldsymbol{x} + \boldsymbol{C}_v\dot{\boldsymbol{x}} + \boldsymbol{C}_a\ddot{\boldsymbol{x}} \tag{7}$$

where $\boldsymbol{C}_p$, $\boldsymbol{C}_v$, and $\boldsymbol{C}_a$ respectively represent the output influence matrices of dimensions $n_y \times n_x$ associated with the system generalized displacements, velocities, and accelerations. These output influence matrices are generated taking into account the mathematical relationships between the configuration vectors $\boldsymbol{x}$, $\dot{\boldsymbol{x}}$, and $\ddot{\boldsymbol{x}}$ and the measurement vector $\boldsymbol{y}$. In analogy with the dynamic equations given by Equation (1), the measurement equations given by Equation (7) can be represented in the state-space form by introducing the definition of the state vector, thereby leading to:

$$\boldsymbol{y} = \boldsymbol{C}_c\boldsymbol{z} + \boldsymbol{D}_c\boldsymbol{u} \tag{8}$$

where $\boldsymbol{C}_c$ is the continuous-time output influence matrix of dimensions $n_y \times n_z$ and $\boldsymbol{D}_c$ is the continuous-time direct transmission matrix having dimensions $n_y \times n_u$ that are respectively defined as:

$$\boldsymbol{C}_c = \begin{bmatrix} \boldsymbol{C}_p - \boldsymbol{C}_a\boldsymbol{M}^{-1}\boldsymbol{K} & \boldsymbol{C}_v - \boldsymbol{C}_a\boldsymbol{M}^{-1}\boldsymbol{R} \end{bmatrix}, \quad \boldsymbol{D}_c = \boldsymbol{C}_a\boldsymbol{M}^{-1}\boldsymbol{B}_a \tag{9}$$

In mechanical engineering problems, it is important to note that the direct transmission matrix disappears from the output equations when the accelerometers are not used for obtaining the vibration measurements. Therefore, the system equations of motion and the corresponding measurement equations form the basis of a continuous-time state-space model of the linear dynamical system of interest. This continuous-time state-space dynamical model has a model order equal to n_z, where n_z is the fundamental dimension associated with the system state matrix.

2.2 Discrete-Time State-Space Dynamical Models

In this subsection, a simple transformation process is used for converting the continuous-time state-space representation of the linear dynamical model of a general mechanical system into its discrete-time counterpart [76,77]. In fact, any linear time-invariant mechanical system with discrete inputs can be represented by a discrete-time space-state model. To this end, the system state vector $\boldsymbol{z}$ is discretized in an equispaced fashion along the time axis employing a constant sampling time equal to Δt. By doing so, one can approximate the continuous-time state vector $\boldsymbol{z}$, evaluated at an arbitrary instant of time t, with its discrete counterpart denoted with the vector $\boldsymbol{z}_n$, where the subscript n denotes a generic discrete instant of time corresponding to the continuous-time variable t_n. The same procedure is applied to the continuous-time input and output vectors $\boldsymbol{u}$ and $\boldsymbol{y}$, leading to their corresponding discrete-time counterparts denoted respectively with $\boldsymbol{u}_n$ and $\boldsymbol{y}_n$. Thus, the discretization process yields:

$$t_n = n\Delta t, \quad n = 0, 1, 2, \ldots, N \quad \Rightarrow \quad \begin{cases} \boldsymbol{z}_n = \boldsymbol{z}(t_n) \\ \boldsymbol{u}_n = \boldsymbol{u}(t_n) \\ \boldsymbol{y}_n = \boldsymbol{y}(t_n) \end{cases} \tag{10}$$

where Δt is the discrete time step, $N = \text{floor}(T/\Delta t)$ is the number of discretization points excluding the zero, T is the total time interval, floor(x) is the function that takes as input a real number x and gives as output the greatest integer less than or equal to x, and $l = N + 1$ is the length of the discretized arrays associated with the data records. After performing the discretization process to the vector variables of interest, the discrete-time state-space dynamic model can be obtained from the continuous-time state-space model by applying the Duhamel principle. The Duhamel principle provides the analytical solution of the state-space equations of motion expressed in the continuous-time domain. This analytical method can be mathematically stated as follows:

$$\boldsymbol{z} = e^{\boldsymbol{A}_c(t-t_0)}\boldsymbol{z}_0 + \int_{t_0}^{t} e^{\boldsymbol{A}_c(t-\tau)}\boldsymbol{B}_c\boldsymbol{u}(\tau)d\tau \tag{11}$$

where t_0 is the initial instant of time, $\boldsymbol{z}_0$ is the vector of initial conditions, and τ is a fictitious time variable used for computing the definite time integral. By substituting the discretization of the vector variables of interest into the Duhamel principle, one obtains:

$$\begin{aligned} \boldsymbol{z}_{n+1} &= e^{\boldsymbol{A}_c\Delta t}\boldsymbol{z}_n + \int_{n\Delta t}^{(n+1)\Delta t} e^{\boldsymbol{A}_c((n+1)\Delta t-\tau)}\boldsymbol{B}_c\boldsymbol{u}(\tau)d\tau \\ &= e^{\boldsymbol{A}_c\Delta t}\boldsymbol{z}_n + \int_0^{\Delta t} e^{\boldsymbol{A}_c\bar{\tau}}\boldsymbol{B}_c d\bar{\tau}\boldsymbol{u}_n \end{aligned} \tag{12}$$

where the input vector $\boldsymbol{u}$ is assumed to be constant between the sample times and the new fictitious time variable $\bar{\tau} = (n+1)\,\Delta t - \tau$ is employed for simplifying the calculation of the definite integral. By doing so, one obtains the following discrete-time version of the system equations of motion represented in the space of the states:

$$\boldsymbol{z}_{n+1} = \boldsymbol{A}_d\boldsymbol{z}_n + \boldsymbol{B}_d\boldsymbol{u}_n \tag{13}$$

where $\boldsymbol{A}_d$ denotes the discrete-time system state matrix having dimensions $n_z \times n_z$ and $\boldsymbol{B}_d$ embodies the discrete-time input influence matrix of dimensions $n_z \times n_u$. By adopting the numerical procedure introduced above, these matrices can be respectively determined as follows:

$$\boldsymbol{A}_d = e^{\boldsymbol{A}_c\Delta t}, \quad \boldsymbol{B}_d = \left(\int_0^{\Delta t} e^{\boldsymbol{A}_c\bar{\tau}}d\bar{\tau}\right)\boldsymbol{B}_c \tag{14}$$

The measurement equations, on the other hand, are not affected by the discretization process since these equations are algebraic equations instead of differential equations. Therefore, for the discrete-time output equations, one can readily replace the continuous-time vector variables with their discrete-time counterparts and directly write:

$$\boldsymbol{y}_n = \boldsymbol{C}_d\boldsymbol{z}_n + \boldsymbol{D}_d\boldsymbol{u}_n \tag{15}$$

where $\boldsymbol{C}_d$ is the discrete-time output influence matrix of dimensions $n_y \times n_z$ and $\boldsymbol{D}_d$ is the discrete-time direct transmission matrix having dimensions $n_y \times n_u$, which are both identical to their continuous-time counterparts $\boldsymbol{C}_c$ and $\boldsymbol{D}_c$. These equations constitute the fundamental mathematical relationships that define a discrete-time space-state dynamical model of a mechanical system. Since in practical applications the experimental data are measured in a discrete fashion, this discrete set of state-space equations stands at the base of the construction of each system identification numerical procedure suitable for modeling linear time-invariant dynamical systems.

2.3 System Markov Parameters

In this subsection, a fundamental set of discrete-time matrices that is suitable for the development of system identification numerical procedures based on the time domain is introduced [76,77]. These parameters are associated with a discrete-time state-space dynamical model and are called Markov parameters. The set of Markov parameters forms a sequence of discrete impulse response functions and, therefore, it is also known as the sequence of matrix impulse responses. The set of Markov parameters is useful for defining the time-domain input-output relationships that stand behind the dynamical behavior of linear time-invariant systems. In particular, three different families of discrete sequences can be constructed, namely the system Markov parameters, the observer Markov parameters, and the observer gain Markov parameters. For this purpose, assuming a discrete-time state-space representation of the dynamic equations and the measurement equations, one can write the system time response to an arbitrary input vector as follows:

$$\begin{cases} \boldsymbol{z}_n = \boldsymbol{A}_d^n\boldsymbol{z}_0 + \sum\limits_{h=1}^{n}\left(\boldsymbol{A}_d^{h-1}\boldsymbol{B}_d\boldsymbol{u}_{n-h}\right) \\ \boldsymbol{y}_n = \boldsymbol{C}_d\boldsymbol{A}_d^n\boldsymbol{z}_0 + \boldsymbol{C}_d\sum\limits_{h=1}^{n}\left(\boldsymbol{A}_d^{h-1}\boldsymbol{B}_d\boldsymbol{u}_{n-h}\right) + \boldsymbol{D}_d\boldsymbol{u}_n \end{cases} \tag{16}$$

where $\boldsymbol{z}_0$ denotes a given set of initial conditions. The previous matrix equations represent a general recursive formulation of the system discrete-time state-space model to which an arbitrary set of input functions can be applied. If, for simplicity, a homogeneous set of initial conditions is assumed and a particular set of input functions is considered, such as a sequence of unitary impulse functions applied one by one only at the initial instant of time, one obtains a sequence of matrix responses based on the so-called set of the system Markov parameters. Thus, one can calculate the system impulsive responses as follows:

$$\begin{cases} \boldsymbol{z}_n = \sum\limits_{h=0}^{n}\left(\boldsymbol{Z}_h\boldsymbol{u}_{n-h}\right) \\ \boldsymbol{y}_n = \sum\limits_{h=0}^{n}\left(\boldsymbol{Y}_h\boldsymbol{u}_{n-h}\right) \end{cases} \tag{17}$$

where $\boldsymbol{Z}_n$ and $\boldsymbol{Y}_n$ denote two sequences of discrete impulse response functions described by rectangular matrices having dimensions $n_z \times n_u$ and $n_y \times n_u$, respectively. This set of dynamic parameters identifies the system Markov parameters that can be expressed in the following compact matrix form:

$$\begin{cases} \boldsymbol{Z}_0 = \boldsymbol{O},\ \boldsymbol{Z}_1 = \boldsymbol{B}_d,\ \boldsymbol{Z}_2 = \boldsymbol{A}_d\boldsymbol{B}_d,\ \ldots,\ \boldsymbol{Z}_n = \boldsymbol{A}_d^{n-1}\boldsymbol{B}_d \\ \boldsymbol{Y}_0 = \boldsymbol{D}_d,\ \boldsymbol{Y}_1 = \boldsymbol{C}_d\boldsymbol{B}_d,\ \boldsymbol{Y}_2 = \boldsymbol{C}_d\boldsymbol{A}_d\boldsymbol{B}_d,\ \ldots,\ \boldsymbol{Y}_n = \boldsymbol{C}_d\boldsymbol{A}_d^{n-1}\boldsymbol{B}_d \end{cases} \tag{18}$$

It immediately follows that the two families of system Markov parameters are connected by the following relation:

$$\boldsymbol{Y}_n = \boldsymbol{C}_d\boldsymbol{Z}_n \tag{19}$$

The system Markov parameters stand at the base of the development of different computational procedures for performing the system identification of dynamical models. In fact, the family of Markov parameters associated with the discrete-time measurement equations can be calculated by using a simple least-squares approach based on experimental input-output data sets. Furthermore, it is important to note that the system Markov parameters contain key information on the dynamical behavior of time-invariant discrete-time dynamical systems since they are constructed considering the system response to an impulsive sequence of discrete inputs applied one by one. The system Markov parameters are a unique metric for describing the dynamics of a discrete-time system in which the state-space model is encapsulated. By writing the time response of a dynamical system in terms of the system Markov parameters $\boldsymbol{Z}_n$ and $\boldsymbol{Y}_n$, one can also observe that they represent the weights associated with the system state vector $\boldsymbol{z}_n$ and to the measured output vector $\boldsymbol{y}_n$ at a general discrete time step denoted with n, which are respectively induced by the current input vector $\boldsymbol{u}_n$ and by the input vectors applied at the previous time steps $\boldsymbol{u}_{n-h}$. For this reason, the system Markov parameters are also known as discrete weighting sequence description. The weighting sequence description formed by the system Markov parameters simply defines the input-output relationship of linear dynamical systems in terms of discrete impulse response functions. Thus, the fundamental difference between the dynamical description based on the state-space representation and the dynamical representation founded on the weighting sequence description is that the latter makes use of sequences of impulse response matrices instead of employing a finite set of state matrices as in the former approach. In particular, the advantage of the discrete weighting sequence description over the state-space representation is the compact dimensions of the matrices associated with the system Markov parameters. In particular, the dimensions of the matrix sequence $\boldsymbol{Y}_n$ that appear in the system input-output relationship are induced only by the number of inputs n_u and outputs n_y, independently of the dimensions of the system state vector n_z. However, the set of system Markov parameters, as previously formulated, involves the drawback of requiring a large number of discrete matrices in the input-output sequence in order to be consistent with the dynamic behavior of lightly damped mechanical systems because, in this case, a large number of terms must be retained in the discrete summation. In order to solve this important issue, a viable approach is based on the introduction of an optimal state estimator called observer.

2.4 Observer Markov Parameters and Observer Gain Markov Parameters

In this subsection, two dual sets of Markov parameters are introduced [1,8]. These discrete sequences are respectively called observer Markov parameters and observer gain Markov Parameters. From a mathematical point of view, a state observer is represented by a rectangular matrix aimed at computing an estimation of the system state by filtering the influence of the process and measurement noise. Therefore, since in realistic applications the system state is not directly measurable, or it is only partially tangible, the introduction of the state observer leads to an improvement in the prediction of the dynamical behavior of the linear system of interest by using the information contained in the input-output data set. From a physical viewpoint, the discrete-time state-space dynamical model of the linear system of interest can be rewritten by including the state observer in the following manner:

$$\begin{cases} \hat{\boldsymbol{z}}_{n+1} = \boldsymbol{A}_d \hat{\boldsymbol{z}}_n + \boldsymbol{B}_d \boldsymbol{u}_n + \boldsymbol{L}_d \left(\hat{\boldsymbol{y}}_n - \boldsymbol{y}_n \right) \\ \hat{\boldsymbol{y}}_n = \boldsymbol{C}_d \hat{\boldsymbol{z}}_n + \boldsymbol{D}_d \boldsymbol{u}_n \end{cases} \tag{20}$$

where $\boldsymbol{L}_d$ denotes a rectangular matrix of dimensions $n_u + n_y$ associated with the state observer. Equation (20) immediately leads to:

$$\begin{cases} \hat{\boldsymbol{z}}_{n+1} = \bar{\boldsymbol{A}}_d \hat{\boldsymbol{z}}_n + \bar{\boldsymbol{B}}_d \boldsymbol{v}_n \\ \hat{\boldsymbol{y}}_n = \boldsymbol{C}_d \hat{\boldsymbol{z}}_n + \boldsymbol{D}_d \boldsymbol{u}_n \end{cases} \tag{21}$$

where $\hat{\boldsymbol{z}}_n$ identifies the state vector having dimension n_z estimated by means of the observer, $\hat{\boldsymbol{y}}_n$ represents the measurement vector of dimension n_y estimated employing of the observer, $\bar{\boldsymbol{A}}_d$ is the modified discrete-time state matrix having dimensions $n_z \times n_z$, $\bar{\boldsymbol{B}}_d$ is the modified discrete-time state influence matrix of dimensions $n_z \times (n_u + n_y)$, and $\boldsymbol{v}(k)$ denotes the generalized input vector having dimension $n_u + n_y$ modified by the introduction of the observer. These matrix and vector quantities are respectively given by:

$$\bar{\boldsymbol{A}}_d = \boldsymbol{A}_d + \boldsymbol{L}_d \boldsymbol{C}_d, \quad \bar{\boldsymbol{B}}_d = \begin{bmatrix} \boldsymbol{B}_d + \boldsymbol{L}_d \boldsymbol{D}_d & -\boldsymbol{L}_d \end{bmatrix} \tag{22}$$

and

$$\boldsymbol{v}_n = \begin{bmatrix} \boldsymbol{u}_n \\ \boldsymbol{y}_n \end{bmatrix} \tag{23}$$

It this, therefore, apparent that the introduction of a state estimator leads to a linear discrete-time state-space observer dynamical model having a mathematical structure that is identical to the original time-invariant discrete-time state-space model. In the resulting mathematical model, the main goal of the state estimator $\boldsymbol{L}_d$ is to conveniently change the eigenvalues of the modified state matrix $\bar{\boldsymbol{A}}_d$ called the observer state matrix. By doing so, the discrete-time state-space observer dynamical model produces compact time histories of the observed state vector $\hat{\boldsymbol{z}}_n$ that can be properly used for the deriving the time evolutions of the original state vector $\boldsymbol{z}_n$. More importantly, the state observer $\boldsymbol{L}_d$ works also as a dynamic filter which reduces the influence of the process and measurement noise, leading to an improvement of the numerical results obtained from actual experimental measurements. It is worth to note that the discrete-time state-space dynamical model associated with the state estimator is mathematically identical to the original discrete-time state-space dynamical model. Thus, in analogy with the previous case, one can introduce another weighting sequence description based on the so-called observer Markov parameters. The observer Markov parameters are defined in the following sequential form:

$$\begin{cases} \bar{\boldsymbol{Z}}_0 = \boldsymbol{O},\ \bar{\boldsymbol{Z}}_1 = \bar{\boldsymbol{B}}_d,\ \bar{\boldsymbol{Z}}_2 = \bar{\boldsymbol{A}}_d \bar{\boldsymbol{B}}_d,\ \dots,\ \bar{\boldsymbol{Z}}_n = \bar{\boldsymbol{A}}_d^{n-1} \bar{\boldsymbol{B}}_d \\ \bar{\boldsymbol{Y}}_0 = \boldsymbol{D}_d,\ \bar{\boldsymbol{Y}}_1 = \boldsymbol{C}_d \bar{\boldsymbol{B}}_d,\ \bar{\boldsymbol{Y}}_2 = \boldsymbol{C}_d \bar{\boldsymbol{A}}_d \bar{\boldsymbol{B}}_d,\ \dots,\ \bar{\boldsymbol{Y}}_n = \boldsymbol{C}_d \bar{\boldsymbol{A}}_d^{n-1} \bar{\boldsymbol{B}}_d \end{cases} \tag{24}$$

where $\bar{\boldsymbol{Z}}_n$ denotes a rectangular matrix of dimensions $n_z \times (n_u + n_y)$ and $\bar{\boldsymbol{Y}}_n$ represents another rectangular matrix having dimensions $n_y \times (n_u + n_y)$ which form the sequences of the observer Markov parameters. At each time step, these discrete sets of dynamic parameters satisfy the following restriction:

$$\bar{\boldsymbol{Y}}_n = \boldsymbol{C}_d \bar{\boldsymbol{Z}}_n \tag{25}$$

On the other hand, one can conveniently partition the two sequences of the observer Markov parameters $\bar{\boldsymbol{Z}}_n$ and $\bar{\boldsymbol{Y}}_n$ in matrix blocks to yield:

$$\bar{\boldsymbol{Z}}_n = \begin{bmatrix} \bar{\boldsymbol{Z}}_n^I & -\bar{\boldsymbol{Z}}_n^{II} \end{bmatrix}, \quad \bar{\boldsymbol{Y}}_n = \begin{bmatrix} \bar{\boldsymbol{Y}}_n^I & -\bar{\boldsymbol{Y}}_n^{II} \end{bmatrix} \tag{26}$$

where $\bar{\boldsymbol{Z}}_n^I$, $\bar{\boldsymbol{Z}}_n^{II}$, $\bar{\boldsymbol{Y}}_n^I$, and $\bar{\boldsymbol{Y}}_n^{II}$ denote rectangular matrices of the observer Markov parameters of dimensions $n_z \times n_u$, $n_z \times n_y$, $n_y \times n_u$, and $n_y \times n_y$, respectively. These matrix quantities are respectively given by:

$$\bar{\boldsymbol{Z}}_n^I = (\boldsymbol{A}_d + \boldsymbol{L}_d\boldsymbol{C}_d)^{n-1}(\boldsymbol{B}_d + \boldsymbol{L}_d\boldsymbol{D}_d),\ \bar{\boldsymbol{Z}}_n^{II} = (\boldsymbol{A}_d + \boldsymbol{L}_d\boldsymbol{C}_d)^{n-1}\boldsymbol{L}_d \tag{27}$$

and

$$\bar{\boldsymbol{Y}}_n^I = \boldsymbol{C}_d(\boldsymbol{A}_d + \boldsymbol{L}_d\boldsymbol{C}_d)^{n-1}(\boldsymbol{B}_d + \boldsymbol{L}_d\boldsymbol{D}_d),\ \bar{\boldsymbol{Y}}_n^{II} = \boldsymbol{C}_d(\boldsymbol{A}_d + \boldsymbol{L}_d\boldsymbol{C}_d)^{n-1}\boldsymbol{L}_d \tag{28}$$

where:

$$\bar{\boldsymbol{Y}}_n^I = \boldsymbol{C}_d\bar{\boldsymbol{Z}}_n^I,\quad \bar{\boldsymbol{Y}}_n^{II} = \boldsymbol{C}_d\bar{\boldsymbol{Z}}_n^{II} \tag{29}$$

Another important advantage associated with the use of the observer Markov parameters relies on the fact that the original system Markov parameters are amenable to be calculated from the former set of sequential parameters. Thus, general purpose system identification numerical algorithms can be specifically designed by employing as input data the observer Markov parameters $\bar{\boldsymbol{Z}}_n$ and $\bar{\boldsymbol{Y}}_n$ instead of the system Markov parameters $\boldsymbol{Z}_n$ and $\boldsymbol{Y}_n$. Assuming a homogeneous set of initial conditions, the estimated state vector $\hat{\boldsymbol{z}}_n$ and the observed measurement vector $\hat{\boldsymbol{y}}_n$ can be recursively derived from the time history of the augmented input vector $\boldsymbol{v}_n$ by using the definition of the observer Markov parameters as follows:

$$\begin{cases} \hat{\boldsymbol{z}}_n = \sum_{h=0}^{n} \left(\bar{\boldsymbol{Z}}_h\boldsymbol{v}_{n-h}\right) \\ \hat{\boldsymbol{y}}_n = \sum_{h=0}^{n} \left(\bar{\boldsymbol{Y}}_h\boldsymbol{v}_{n-h}\right) \end{cases} \tag{30}$$

One can also explicitly write the observed measurement vector $\hat{\boldsymbol{y}}_n$ in terms of the block matrices $\bar{\boldsymbol{Y}}_n^I$ and $\bar{\boldsymbol{Y}}_n^{II}$ arising from the partitioning of the observer Markov parameters $\bar{\boldsymbol{Y}}_n$ to yield:

$$\hat{\boldsymbol{y}}_n + \sum_{h=1}^{n}\left(\bar{\boldsymbol{Y}}_h^{II}\boldsymbol{y}_{n-h}\right) = \sum_{h=1}^{n}\left(\bar{\boldsymbol{Y}}_h^{I}\boldsymbol{u}_{n-h}\right) + \boldsymbol{D}_d\boldsymbol{u}_n \tag{31}$$

As mentioned before, the structure of the observer state matrix $\bar{\boldsymbol{A}}_d$ is significantly influenced by the introduction of the state observer matrix $\boldsymbol{L}_d$. In particular, one can devise an appropriate state observer identified by the discrete gain matrix $\boldsymbol{L}_d$ such that the matrix power $\bar{\boldsymbol{A}}_d^p$ quickly approaches the null matrix considering a small integer exponential p. This reasoning implies that, if the rectangular matrix of the observer is properly designed, one can retain only the first few p terms in the summations used for computing the observed state vector $\hat{\boldsymbol{z}}_n$ and the estimated output vector $\hat{\boldsymbol{y}}_n$. This approach is efficient and effective in the resolution of practical system identification problems because it leads to the use of smaller input-output data sets. By doing so, one can write:

$$\hat{\boldsymbol{y}}_n + \sum_{h=1}^{p}\left(\bar{\boldsymbol{Y}}_h^{II}\boldsymbol{y}_{n-h}\right) = \sum_{h=1}^{p}\left(\bar{\boldsymbol{Y}}_h^{I}\boldsymbol{u}_{n-h}\right) + \boldsymbol{D}_d\boldsymbol{u}_n \tag{32}$$

where p is an integer number associated with the selection of the matrix of the state observer $\boldsymbol{L}_d$ that is smaller than the current number of time steps n. The resulting observer weighting sequence description forms a linear difference model associated with the discrete-time state-space dynamical model of the system under consideration. An effective approach for computing the coefficients of the observer linear difference model is to resort to the definition of another sequential set of Markov parameters called observer gain Markov parameters. The observer gain Markov parameters represent a dual set of observer Markov parameters defined as:

$$\begin{cases} \boldsymbol{Z}_1^0 = \boldsymbol{L}_d,\ \boldsymbol{Z}_2^0 = \boldsymbol{A}_d\boldsymbol{L}_d,\ \dots,\ \boldsymbol{Z}_n^0 = \boldsymbol{A}_d^{n-1}\boldsymbol{L}_d \\ \boldsymbol{Y}_1^0 = \boldsymbol{C}_d\boldsymbol{L}_d,\ \boldsymbol{Y}_2^0 = \boldsymbol{C}_d\boldsymbol{A}_d\boldsymbol{L}_d,\ \dots,\ \boldsymbol{Y}_n^0 = \boldsymbol{C}_d\boldsymbol{A}_d^{n-1}\boldsymbol{L}_d \end{cases} \tag{33}$$

where $\boldsymbol{Z}_n^0$ identifies a rectangular matrix having dimensions $n_z \times n_y$ and $\boldsymbol{Y}_n^0$ indicates another rectangular matrix of dimensions $n_y \times n_y$ that constitutes the sequences of observer gain Markov parameters. As in the cases of the system Markov parameters and the observer Markov parameters, it is straightforward to prove that the observer gain Markov parameters comply with the following simple relation:

$$\boldsymbol{Y}_n^0 = \boldsymbol{C}_d\boldsymbol{Z}_n^0 \tag{34}$$

Essentially, the observer gain Markov parameters represent an auxiliary sequential set of discrete parameters useful for facilitating the process of the system identification in the sense that they allow for estimating the matrix of the state observer in conjunction with the system state-space dynamical model. Moreover, the system Markov parameters and the observer gain Markov parameters can be recovered from an identified set of observer Markov parameters by means of a simple least-squares estimation procedure directly based on the measurement of input and output data. Subsequently, one can conveniently use the set of the system Markov parameters and the set of the observer gain Markov parameters in combination with a general system identification approach.

2.5 Computation of the Markov Parameters

In this subsection, a least-squares method based on the use of the Moore-Penrose generalized inverse matrix is used for the computation of the sequence of the system Markov parameters together with the observer gain Markov parameters starting from experimental input and output data [1, 8]. The straightforward numerical procedure discussed in this section also leads to the determination of the set of the observer Markov parameters. In order to achieve this goal, the starting point is the establishment of the weighting sequence description associated with the observer Markov parameters given by:

$$\hat{\boldsymbol{y}}_n \simeq \boldsymbol{y}_n \quad \Rightarrow \quad \boldsymbol{y}_n = \sum_{h=0}^{p}\left(\bar{\boldsymbol{Y}}_h\boldsymbol{v}_{n-j}\right) \tag{35}$$

where the estimated measurement vector $\hat{\boldsymbol{y}}_n$ is assumed to be sufficiently close to the actual output $\boldsymbol{y}_n$ vector and, therefore, only the first p terms are considered in the summation. The previous weighting description can be conveniently rearranged to construct an assembled matrix equation amenable to be treated by means of a least-squares approach for the determination of the coefficients that appear in the linear difference model. For this purpose, one can simply write:

$$\boldsymbol{Y} = \tilde{\boldsymbol{Y}}_p \boldsymbol{V}_p \tag{36}$$

where $\boldsymbol{Y}$ is a rectangular matrix having dimensions $n_y \times l$ constitute of output vectors, $\tilde{\boldsymbol{Y}}_p$ is a rectangular matrix of dimensions $n_y \times (n_u + p(n_u + n_y))$ formed by the observer Markov parameters, $\boldsymbol{V}_p$ is a rectangular matrix having dimensions $(n_u + p(n_u + n_y)) \times l$ made of input and output vectors, and l is the length of the data acquisition. These matrix quantities can be respectively assembled as follows:

$$\begin{cases} \boldsymbol{Y} = \begin{bmatrix} \boldsymbol{y}_0 & \boldsymbol{y}_1 & \boldsymbol{y}_2 & \dots & \boldsymbol{y}_{l-1} \end{bmatrix} \\ \tilde{\boldsymbol{Y}}_p = \begin{bmatrix} \bar{\boldsymbol{Y}}_0 & \bar{\boldsymbol{Y}}_1 & \bar{\boldsymbol{Y}}_2 & \dots & \bar{\boldsymbol{Y}}_p \end{bmatrix} \end{cases} \tag{37}$$

and

$$\boldsymbol{V}_p = \begin{bmatrix} \boldsymbol{u}_0 & \boldsymbol{u}_1 & \dots & \boldsymbol{u}_p & \dots & \boldsymbol{u}_{l-1} \\ \boldsymbol{0} & \boldsymbol{v}_0 & \dots & \boldsymbol{v}_{p-1} & \dots & \boldsymbol{v}_{l-2} \\ \vdots & \vdots & \ddots & \vdots & \dots & \vdots \\ \boldsymbol{0} & \boldsymbol{0} & \dots & \boldsymbol{v}_0 & \dots & \boldsymbol{v}_{l-p-1} \end{bmatrix} \tag{38}$$

Note that only the first p observer Markov parameters are considered in this simple estimation numerical algorithm and, therefore, the integer number p plays the important role of a fundamental tuning parameter. By assuming a least-square estimation strategy based on the use of the Moore-Penrose generalized inverse matrix, one can directly write:

$$\boldsymbol{P}_p = \boldsymbol{V}_p^+ \quad \Rightarrow \quad \tilde{\boldsymbol{Y}}_p = \boldsymbol{Y}\boldsymbol{P}_p \tag{39}$$

where the rectangular matrix $\boldsymbol{P}_p$ of dimensions $l \times (n_u + p(n_u + n_y))$ is the Moore-Penrose pseudoinverse matrix associated with the known matrix $\boldsymbol{V}_p$ as indicated by the plus superscript. One viable approach for computing the pseudoinverse matrix $\boldsymbol{P}_p$ is to exploit the Singular Value Decomposition (SVD) of the coefficient matrix $\boldsymbol{V}_p$ and this strategy represents the standard computation approach employed in the literature [78]. Furthermore, once the observer Markov parameters contained in the block matrix $\tilde{\boldsymbol{Y}}_p$ are obtained, one can readily employ a recursive computational approach for determining the system Markov parameters and the observer gain Markov parameters. To this end, the following set of equations are suitable for performing this fundamental task:

$$\begin{cases} \boldsymbol{D}_d = \boldsymbol{Y}_0 = \bar{\boldsymbol{Y}}_0, \quad n = 0 \\ \boldsymbol{Y}_n = \bar{\boldsymbol{Y}}_n^I - \sum\limits_{h=1}^{n} \bar{\boldsymbol{Y}}_h^{II} \boldsymbol{Y}_{n-h}, \quad n = 1, 2, \dots, p \\ \boldsymbol{Y}_n = -\sum\limits_{h=1}^{p} \bar{\boldsymbol{Y}}_h^{II} \boldsymbol{Y}_{n-h}, \quad n = p+1, p+2, \dots \end{cases} \tag{40}$$

and

$$\begin{cases} \boldsymbol{Y}_1^0 = \boldsymbol{C}_d \boldsymbol{L}_d = \bar{\boldsymbol{Y}}_1^{II}, \quad n = 1 \\ \boldsymbol{Y}_n^0 = \bar{\boldsymbol{Y}}_n^{II} - \sum\limits_{h=1}^{n-1} \bar{\boldsymbol{Y}}_h^{II} \boldsymbol{Y}_{n-h}^0, \quad n = 2, 3, \dots, p \\ \boldsymbol{Y}_n^0 = -\sum\limits_{h=1}^{p} \bar{\boldsymbol{Y}}_h^{II} \boldsymbol{Y}_{n-h}^0, \quad n = p+1, p+2, \dots \end{cases} \tag{41}$$

One can prove that the previous recursive equations originate from simple matrix manipulations of the definition of the system Markov parameters as well as the observer Markov parameters [1]. Another important point to be emphasized is the fact that the choice of the integer parameter p, which is typically left to the experience of the analyst, has a fundamental impact on the quality of the identified sets of Markov parameters. Moreover, based on constructive considerations on the formulation of the observer Markov parameters, the integer parameter p must satisfy the limit $n_y p \geq n_z$. The integer parameter p can also be directly interpreted as the number of independent Markov parameters retained in the discrete approximation of the system state-space model.

3. Time-Domain System Identification Methods

In this section, the principal features of the methodologies for performing the system identification of linear dynamical systems in the time domain are described. To this end, two fundamentally diverse computational procedures are considered. The first approach of interest is based on the Eigensystem Realization Algorithm (ERA) combined with the Observer/Kalman Filter Identification Methods (OKID), while the second approach considered is founded on the Numerical Algorithms for Subspace State-Space System Identification (N4SID). Subsequently, a method for carrying out the Mass, Stiffness, and Damping Matrices identification (MKR) is discussed and an effective least-square strategy for the Proportional Damping Coefficients identification (PDC) is proposed.

3.1 Eigensystem Realization Algorithm (ERA) and Observer/Kalman Filter Identification Methods (OKID)

In this subsection, the key points of the identification technique based on the Eigensystem Realization Algorithm (ERA) with the Observer/Kalman Filter Identification methods (OKID) are illustrated in detail [79,80]. This method is used to recover the state-space matrices of a linear dynamical system with the use of the system Markov parameters, the observer Markov parameters, and the observer gain Markov parameters computed for the mechanical system of interest. To this end, the combination of the system Markov parameters denoted with $\boldsymbol{Y}_k$ with the observer gain Markov parameters denoted with $\boldsymbol{Y}_k^0$ is exploited by using the assembled matrix denoted with $\boldsymbol{\Gamma}_k$ and given by:

$$\boldsymbol{\Gamma}_k = \begin{bmatrix} \boldsymbol{Y}_k & \boldsymbol{Y}_k^0 \end{bmatrix} \tag{42}$$

where $\boldsymbol{\Gamma}_k$ is a rectangular matrix having dimensions $n_y \times (n_u + n_y)$ that is referred to as the combined matrix of Markov parameters. Thus, the generalized block Hankel matrix indicated as $\boldsymbol{H}(k-1)$ is defined using the assembled matrix denoted with $\boldsymbol{\Gamma}_k$ as follows:

$$\boldsymbol{H}(k-1) = \begin{bmatrix} \boldsymbol{\Gamma}_k & \boldsymbol{\Gamma}_{k+1} & \cdots & \boldsymbol{\Gamma}_{k+\gamma-1} \\ \boldsymbol{\Gamma}_{k+1} & \boldsymbol{\Gamma}_{k+2} & \cdots & \boldsymbol{\Gamma}_{k+\gamma} \\ \vdots & \vdots & \ddots & \vdots \\ \boldsymbol{\Gamma}_{k+p-1} & \boldsymbol{\Gamma}_{k+p} & \cdots & \boldsymbol{\Gamma}_{k+p+\gamma-2} \end{bmatrix} \tag{43}$$

where $\boldsymbol{H}(k-1)$ is a rectangular matrix having dimensions $pn_y \times \gamma(n_u + n_y)$ that is referred to as the generalized block Hankel matrix, while p and γ are appropriate integer numbers. For $k = 1$, one obtains the Hankel matrix denoted with $\boldsymbol{H}(0)$, which can be explicitly written as:

$$\boldsymbol{H}(0) = \begin{bmatrix} \boldsymbol{\Gamma}_1 & \boldsymbol{\Gamma}_2 & \cdots & \boldsymbol{\Gamma}_{\gamma} \\ \boldsymbol{\Gamma}_2 & \boldsymbol{\Gamma}_3 & \cdots & \boldsymbol{\Gamma}_{\gamma+1} \\ \vdots & \vdots & \ddots & \vdots \\ \boldsymbol{\Gamma}_p & \boldsymbol{\Gamma}_{p+1} & \cdots & \boldsymbol{\Gamma}_{p+\gamma-1} \end{bmatrix} = \boldsymbol{P}_p \boldsymbol{Q}_{\gamma} \tag{44}$$

where the matrices $\boldsymbol{P}_p$ and $\boldsymbol{Q}_{\gamma}$ are rectangular matrices of dimensions $pn_y \times n_z$ and $n_z \times \gamma(n_u + n_y)$ that respectively represent the observability and the controllability matrices of the dynamical system. These matrices are respectively given by:

$$\boldsymbol{P}_p = \begin{bmatrix} \boldsymbol{C}_d \\ \boldsymbol{C}_d \boldsymbol{A}_d \\ \boldsymbol{C}_d \boldsymbol{A}_d^2 \\ \vdots \\ \boldsymbol{C}_d \boldsymbol{A}_d^{p-1} \end{bmatrix} \tag{45}$$

and

$$\boldsymbol{Q}_{\gamma} = \begin{bmatrix} \tilde{\boldsymbol{B}}_d & \boldsymbol{A}_d \tilde{\boldsymbol{B}}_d & \boldsymbol{A}_d^2 \tilde{\boldsymbol{B}}_d & \cdots & \boldsymbol{A}_d^{\gamma-1} \tilde{\boldsymbol{B}}_d \end{bmatrix} \tag{46}$$

where the rectangular matrix having dimensions $n_z \times (n_u + n_y)$ denoted with $\tilde{\boldsymbol{B}}_d$ consists of a combination of the system input influence matrix $\boldsymbol{B}_d$ and the observer matrix $\boldsymbol{L}_d$. This matrix is defined as follows:

$$\tilde{\boldsymbol{B}}_d = \begin{bmatrix} \boldsymbol{B}_d & \boldsymbol{L}_d \end{bmatrix} \tag{47}$$

Subsequently, the generalized Hankel matrix denoted with $\boldsymbol{H}(0)$ can be readily factorized using the Singular Value Decomposition (SVD) method as follows:

$$\boldsymbol{H}(0) = \boldsymbol{R} \boldsymbol{\Sigma} \boldsymbol{S}^T \tag{48}$$

where $\boldsymbol{R}$ and $\boldsymbol{S}$ are square orthonormal matrices arising from the matrix factorization having respectively dimensions $pn_y \times pn_y$ and $\gamma(n_u + n_y) \times \gamma(n_u + n_y)$, while the non-zero rectangular matrix denoted with $\boldsymbol{\Sigma}$ of dimensions $pn_y \times \gamma(n_u + n_y)$ is given by:

$$\boldsymbol{\Sigma} = \begin{bmatrix} \boldsymbol{\Sigma}_{\hat{n}_z} & \boldsymbol{O} \\ \boldsymbol{O} & \boldsymbol{O} \end{bmatrix} \tag{49}$$

where $\boldsymbol{O}$ is the zero matrix having appropriate dimensions and $\boldsymbol{\Sigma}_{n_z}$ is a square diagonal matrix of dimensions $\hat{n}_z \times \hat{n}_z$ simply defined as follows:

$$\boldsymbol{\Sigma}_{\hat{n}_z} = \text{diag}(\sigma_1, \sigma_2, \ldots, \sigma_{\hat{n}_z}) \tag{50}$$

where $\sigma_i,\ i = 1, 2, \ldots, \hat{n}_z$ represent the identified singular values of the Hankel matrix $\boldsymbol{H}(0)$ and $\hat{n}_z$ denotes the number of the identified singular values, which also corresponds to the dimension of the identified state-space model. Additionally, one can write:

$$\boldsymbol{H}(0) = \boldsymbol{R}_{\hat{n}_z} \boldsymbol{\Sigma}_{\hat{n}_z} \boldsymbol{S}_{\hat{n}_z}^T, \quad \boldsymbol{H}^+(0) = \boldsymbol{S}_{\hat{n}_z} \boldsymbol{\Sigma}_{\hat{n}_z}^{-1} \boldsymbol{R}_{\hat{n}_z}^T \tag{51}$$

where $\boldsymbol{R}_{\hat{n}_z}$ and $\boldsymbol{S}_{\hat{n}_z}$ indicate the rectangular matrices composed of the first $\hat{n}_z$ columns of the matrices $\boldsymbol{R}$ and $\boldsymbol{S}$, whereas $\boldsymbol{H}^+(0)$ is a rectangular matrix of dimensions $\gamma(n_u + n_y) \times pn_y$ representing the Moore-Penrose pseudoinverse matrix of the matrix $\boldsymbol{H}(0)$. Subsequently, the Hankel matrix can be mathematically manipulated to obtain the observability and controllability matrices as follows:

$$\boldsymbol{H}(0) = \left(\boldsymbol{R}_{\hat{n}_z} \boldsymbol{\Sigma}_{\hat{n}_z}^{1/2}\right)\left(\boldsymbol{\Sigma}_{\hat{n}_z}^{1/2} \boldsymbol{S}_{\hat{n}_z}^T\right) = \hat{\boldsymbol{P}}_p \hat{\boldsymbol{Q}}_{\gamma} \quad \Rightarrow \quad \begin{cases} \hat{\boldsymbol{P}}_p = \boldsymbol{R}_{\hat{n}_z} \boldsymbol{\Sigma}_{\hat{n}_z}^{1/2} \\ \\ \hat{\boldsymbol{Q}}_{\gamma} = \boldsymbol{\Sigma}_{\hat{n}_z}^{1/2} \boldsymbol{S}_{\hat{n}_z}^T \end{cases} \tag{52}$$

where $\hat{\boldsymbol{P}}_p$ represents the identified observability matrix and $\hat{\boldsymbol{Q}}_{\gamma}$ represents the identified controllability matrix. By doing so, the identified version of the system input influence matrix $\hat{\boldsymbol{B}}_d$ can be obtained by extracting the first n_u columns of the identified version of the controllability matrix $\hat{\boldsymbol{Q}}_{\gamma}$, while the identified version of the system output influence matrix $\hat{\boldsymbol{C}}_d$ can be obtained by extracting the first n_y rows of the identified version of the observability matrix $\hat{\boldsymbol{P}}_p$. To also calculate the identified version of the system state matrix $\hat{\boldsymbol{A}}_d$, the Hankel matrix calculated for $k = 2$ is denoted with $\boldsymbol{H}(1)$ and can be determined as follows:

$$\boldsymbol{H}(1) = \begin{bmatrix} \boldsymbol{\Gamma}_2 & \boldsymbol{\Gamma}_3 & \cdots & \boldsymbol{\Gamma}_{\gamma+1} \\ \boldsymbol{\Gamma}_3 & \boldsymbol{\Gamma}_4 & \cdots & \boldsymbol{\Gamma}_{\gamma+2} \\ \vdots & \vdots & \ddots & \vdots \\ \boldsymbol{\Gamma}_{p+1} & \boldsymbol{\Gamma}_{p+2} & \cdots & \boldsymbol{\Gamma}_{p+\gamma} \end{bmatrix} = \boldsymbol{P}_p \boldsymbol{A}_d \boldsymbol{Q}_{\gamma} \tag{53}$$

Finally, by using the Markov parameters based on the measured input-output data and the factorization of the generalized Hankel matrix previously introduced, the identified version of the discrete-time state-space matrices of the mechanical system can be explicitly calculated using the ERA-OKID method as follows:

$$\begin{cases} \hat{\boldsymbol{A}}_d = \boldsymbol{\Sigma}_{\hat{n}_z}^{-1/2} \boldsymbol{R}_{\hat{n}_z}^T \boldsymbol{H}(1) \boldsymbol{S}_{\hat{n}_z} \boldsymbol{\Sigma}_{\hat{n}_z}^{-1/2} \\ \begin{bmatrix} \hat{\boldsymbol{B}}_d & \hat{\boldsymbol{L}}_d \end{bmatrix} = \boldsymbol{\Sigma}_{\hat{n}_z}^{1/2} \boldsymbol{S}_{\hat{n}_z}^T \boldsymbol{E}_{n_u+n_y} \\ \hat{\boldsymbol{C}}_d = \boldsymbol{E}_{n_y}^T \boldsymbol{R}_{\hat{n}_z} \boldsymbol{\Sigma}_{\hat{n}_z}^{1/2} \\ \hat{\boldsymbol{D}}_d = \boldsymbol{Y}_0 \end{cases} \tag{54}$$

where $\hat{\boldsymbol{A}}_d$ is the identified discrete-time state matrix, $\hat{\boldsymbol{B}}_d$ is the identified discrete-time input influence matrix, $\hat{\boldsymbol{C}}_d$ is the identified discrete-time output influence matrix, $\hat{\boldsymbol{D}}_d$ is the identified discrete-time direct transmission matrix, $\hat{\boldsymbol{L}}_d$ is the identified discrete-time observer matrix, while $\boldsymbol{E}_{n_y}$ and $\boldsymbol{E}_{n_u+n_y}$ are appropriate Boolean matrices for the dynamical system under consideration.

3.2 Numerical Algorithms for Subspace State-Space System Identification (N4SID)

In this subsection, the main features of the identification method based on the Numerical Algorithms for Subspace State-Space System Identification (N4SID) are explained in detail [3,5]. For this purpose, a discrete-time state-space model of a linear mechanical system, considering its first-order dynamic and measurement equations respectively given by Equation (13) together with Equation (15), can be conveniently rewritten as follows:

$$\begin{cases} \boldsymbol{Y}_p = \boldsymbol{\Gamma}_i \boldsymbol{Z}_p + \boldsymbol{H}_i \boldsymbol{U}_p \\ \boldsymbol{Y}_f = \boldsymbol{\Gamma}_i \boldsymbol{Z}_f + \boldsymbol{H}_i \boldsymbol{U}_f \\ \boldsymbol{Z}_f = \boldsymbol{A}_d^i \boldsymbol{Z}_p + \boldsymbol{\Delta}_i \boldsymbol{U}_p \end{cases} \tag{55}$$

where l is the length of the array containing the recorded data, i and j represent two integer numbers, $\boldsymbol{\Gamma}_i$ denotes the observability matrix having dimensions $in_y \times n_z$, $\boldsymbol{\Delta}_i$ denotes the controllability matrix having dimensions $n_z \times in_u$, and $\boldsymbol{H}_i$ identifies the discrete-time state-space Toeplitz matrix having dimensions $in_y \times in_u$. Also, the rectangular matrices denoted with $\boldsymbol{U}_p$, $\boldsymbol{U}_f$, $\boldsymbol{Y}_p$, and $\boldsymbol{Y}_f$, having respectively dimensions $in_u \times j$, $in_u \times j$, $in_y \times j$, and $in_y \times j$, represent, respectively, the Hankel matrix of the past and future inputs, as well as the Hankel matrix of the past and future outputs. Exploiting the recorded structure of the data set embedded in the input and output vectors, respectively denoted with $\boldsymbol{u}_k$ and $\boldsymbol{y}_k$ for a generic discrete time instant indicated with k, one can assemble all the discrete-time matrices mentioned before as follows:

$$\boldsymbol{U}_p = \begin{bmatrix} \boldsymbol{u}_0 & \boldsymbol{u}_1 & \dots & \boldsymbol{u}_{j-1} \\ \boldsymbol{u}_1 & \boldsymbol{u}_2 & \dots & \boldsymbol{u}_j \\ \vdots & \vdots & \ddots & \vdots \\ \boldsymbol{u}_{i-1} & \boldsymbol{u}_i & \dots & \boldsymbol{u}_{i+j-2} \end{bmatrix} \tag{56}$$

$$\boldsymbol{U}_f = \begin{bmatrix} \boldsymbol{u}_i & \boldsymbol{u}_{i+1} & \dots & \boldsymbol{u}_{i+j-1} \\ \boldsymbol{u}_{i+1} & \boldsymbol{u}_{i+2} & \dots & \boldsymbol{u}_{i+j} \\ \vdots & \vdots & \ddots & \vdots \\ \boldsymbol{u}_{2i-1} & \boldsymbol{u}_{2i} & \dots & \boldsymbol{u}_{2i+j-2} \end{bmatrix} \tag{57}$$

$$\boldsymbol{Y}_p = \begin{bmatrix} \boldsymbol{y}_0 & \boldsymbol{y}_1 & \dots & \boldsymbol{y}_{j-1} \\ \boldsymbol{y}_1 & \boldsymbol{y}_2 & \dots & \boldsymbol{y}_j \\ \vdots & \vdots & \ddots & \vdots \\ \boldsymbol{y}_{i-1} & \boldsymbol{y}_i & \dots & \boldsymbol{y}_{i+j-2} \end{bmatrix} \tag{58}$$

$$\boldsymbol{Y}_f = \begin{bmatrix} \boldsymbol{y}_i & \boldsymbol{y}_{i+1} & \dots & \boldsymbol{y}_{i+j-1} \\ \boldsymbol{y}_{i+1} & \boldsymbol{y}_{i+2} & \dots & \boldsymbol{y}_{i+j} \\ \vdots & \vdots & \ddots & \vdots \\ \boldsymbol{y}_{2i-1} & \boldsymbol{y}_{2i} & \dots & \boldsymbol{y}_{2i+j-2} \end{bmatrix} \tag{59}$$

In principle, the parameters i and j can be selected arbitrarily. However, the larger is the length l of the data record, as well as the dimension of the parameters i and j, the better is the quality of the estimation of the discrete-time state-space model. Additionally, the matrix $\boldsymbol{Z}_p$ of dimensions $n_z \times j$ and the matrix $\boldsymbol{Z}_f$ of dimensions $n_z \times j$ respectively represent the sequences of past and future states. These matrices are constructed as follows:

$$\boldsymbol{Z}_p = \begin{bmatrix} \boldsymbol{z}_0 & \boldsymbol{z}_1 & \dots & \boldsymbol{z}_{j-1} \end{bmatrix} \tag{60}$$

and

$$\boldsymbol{Z}_f = \begin{bmatrix} \boldsymbol{z}_i & \boldsymbol{z}_{i+1} & \dots & \boldsymbol{z}_{i+j-1} \end{bmatrix} \tag{61}$$

The matrix $\boldsymbol{\Gamma}_i$ of dimensions $in_y \times n_z$ and the matrix $\boldsymbol{\Delta}_i$ of dimensions $n_z \times in_u$ respectively represent the observability and controllability matrices. These matrices are assembled as follows:

$$\boldsymbol{\Gamma}_i = \begin{bmatrix} \boldsymbol{C}_d \\ \boldsymbol{C}_d \boldsymbol{A}_d \\ \boldsymbol{C}_d \boldsymbol{A}_d^2 \\ \vdots \\ \boldsymbol{C}_d \boldsymbol{A}_d^{i-1} \end{bmatrix} \tag{62}$$

and

$$\boldsymbol{\Delta}_i = \left[\begin{array}{ccccc} \boldsymbol{A}_d^{i-1}\boldsymbol{B}_d & \boldsymbol{A}_d^{i-2}\boldsymbol{B}_d & \ldots & \boldsymbol{A}_d\boldsymbol{B}_d & \boldsymbol{B}_d \end{array} \right] \tag{63}$$

The triangular Toeplitz matrix denoted with $\boldsymbol{H}_i$ having dimensions $in_y \times in_u$ is explicitly given by:

$$\boldsymbol{H}_i = \left[\begin{array}{ccccc} \boldsymbol{D}_d & \boldsymbol{O} & \boldsymbol{O} & \ldots & \boldsymbol{O} \\ \boldsymbol{C}_d\boldsymbol{B}_d & \boldsymbol{D}_d & \boldsymbol{O} & \ldots & \boldsymbol{O} \\ \boldsymbol{C}_d\boldsymbol{A}_d\boldsymbol{B}_d & \boldsymbol{C}_d\boldsymbol{B}_d & \boldsymbol{D}_d & \ldots & \boldsymbol{O} \\ \vdots & \vdots & \vdots & \ddots & \vdots \\ \boldsymbol{C}_d\boldsymbol{A}_d^{i-2}\boldsymbol{B}_d & \boldsymbol{C}_d\boldsymbol{A}_d^{i-3}\boldsymbol{B}_d & \boldsymbol{C}_d\boldsymbol{A}_d^{i-4}\boldsymbol{B}_d & \ldots & \boldsymbol{D}_d \end{array} \right] \tag{64}$$

where $\boldsymbol{O}$ is a null matrix having appropriate dimensions. The matrix of future states denoted with $\boldsymbol{Z}_f$ can be expressed as a linear combination of the matrices $\boldsymbol{U}_p$ and $\boldsymbol{Y}_p$, respectively representing the matrices of past inputs and past outputs, as follows:

$$\begin{aligned} \boldsymbol{Z}_f &= \boldsymbol{A}_d^i\boldsymbol{Z}_p + \boldsymbol{\Delta}_i\boldsymbol{U}_p = \boldsymbol{A}_d^i\left(\boldsymbol{\Gamma}_i^+\boldsymbol{Y}_p - \boldsymbol{\Gamma}_i^+\boldsymbol{H}_i\boldsymbol{U}_p\right) + \boldsymbol{\Delta}_i\boldsymbol{U}_p \\ &= \left(\boldsymbol{\Delta}_i - \boldsymbol{A}_d^i\boldsymbol{\Gamma}_i^+\boldsymbol{H}_i\right)\boldsymbol{U}_p + \boldsymbol{A}_d^i\boldsymbol{\Gamma}_i^+\boldsymbol{Y}_p = \boldsymbol{L}_p\boldsymbol{W}_p \end{aligned} \tag{65}$$

where the rectangular matrix $\boldsymbol{\Gamma}_i^+$ represents the Moore-Penrose pseudoinverse matrix of the rectangular matrix $\boldsymbol{\Gamma}_i$. The matrices $\boldsymbol{L}_p$ and $\boldsymbol{W}_p$, having respectively dimensions $n_z \times i\,(n_u + n_y)$ and $i\,(n_u + n_y) \times j$, are defined as follows:

$$\boldsymbol{L}_p = \left[\begin{array}{cc} \boldsymbol{\Delta}_i - \boldsymbol{A}_d^i\boldsymbol{\Gamma}_i^+\boldsymbol{H}_i & \boldsymbol{A}_d^i\boldsymbol{\Gamma}_i^+ \end{array} \right], \; \boldsymbol{W}_p = \left[\begin{array}{c} \boldsymbol{U}_p \\ \boldsymbol{Y}_p \end{array} \right] \tag{66}$$

Similarly, the matrix of future outputs denoted with $\boldsymbol{Y}_f$ can be expressed combining Equation (55) with Equation (65) as:

$$\boldsymbol{Y}_f = \boldsymbol{\Gamma}_i\boldsymbol{Z}_f + \boldsymbol{H}_i\boldsymbol{U}_f = \boldsymbol{\Gamma}_i\boldsymbol{L}_p\boldsymbol{W}_p + \boldsymbol{H}_i\boldsymbol{U}_f \tag{67}$$

Let $\boldsymbol{\Pi}_{\boldsymbol{U}_f^\perp}$ be a matrix of dimensions $j \times j$ representing the projection onto the set of future inputs defined as:

$$\boldsymbol{\Pi}_{\boldsymbol{U}_f^\perp} = \boldsymbol{I} - \boldsymbol{U}_f^T\left(\boldsymbol{U}_f\boldsymbol{U}_f^T\right)^+\boldsymbol{U}_f \tag{68}$$

The post-multiplication of the projection matrix $\boldsymbol{\Pi}_{\boldsymbol{U}_f^\perp}$ applied to Equation (67) leads to:

$$\boldsymbol{Y}_f\boldsymbol{\Pi}_{\boldsymbol{U}_f^\perp} = \boldsymbol{\Gamma}_i\boldsymbol{L}_p\boldsymbol{W}_p\boldsymbol{\Pi}_{\boldsymbol{U}_f^\perp}, \quad \boldsymbol{H}_i\boldsymbol{U}_f\boldsymbol{\Pi}_{\boldsymbol{U}_f^\perp} = \boldsymbol{O} \tag{69}$$

Let $\bar{\boldsymbol{W}}_p$ be the following matrix having dimensions $j \times j$:

$$\bar{\boldsymbol{W}}_p = \left(\boldsymbol{W}_p\boldsymbol{\Pi}_{\boldsymbol{U}_f^\perp}\right)^+\boldsymbol{W}_p \tag{70}$$

The post-multiplication of Equation (69) by the matrix denoted with $\bar{\boldsymbol{W}}_p$ leads to:

$$\boldsymbol{Y}_f\boldsymbol{\Pi}_{\boldsymbol{U}_f^\perp}\bar{\boldsymbol{W}}_p = \boldsymbol{\Gamma}_i\boldsymbol{L}_p\boldsymbol{W}_p\boldsymbol{\Pi}_{\boldsymbol{U}_f^\perp}\bar{\boldsymbol{W}}_p \tag{71}$$

Thus, one can write:

$$\boldsymbol{O}_i = \boldsymbol{Y}_f\boldsymbol{\Pi}_{\boldsymbol{U}_f^\perp}\bar{\boldsymbol{W}}_p = \boldsymbol{Y}_f\boldsymbol{\Pi}_{\boldsymbol{U}_f^\perp}\left(\boldsymbol{W}_p\boldsymbol{\Pi}_{\boldsymbol{U}_f^\perp}\right)^+\boldsymbol{W}_p \tag{72}$$

and

$$\boldsymbol{O}_i = \boldsymbol{\Gamma}_i\boldsymbol{L}_p\boldsymbol{W}_p = \boldsymbol{\Gamma}_i\boldsymbol{Z}_f \tag{73}$$

As a final step, the following fundamental matrix equation is deduced:

$$\boldsymbol{O}_i = \boldsymbol{\Gamma}_i\boldsymbol{Z}_f \tag{74}$$

where $\boldsymbol{O}_i$ represents a rectangular matrix of dimensions $in_y \times j$, which can be directly assembled by using the recorded input and output data set. Furthermore, the fundamental matrix denoted with $\boldsymbol{O}_i$ can be readily post-processed by using two appropriate weighting matrices, which are respectively denoted with $\boldsymbol{W}_1$ and $\boldsymbol{W}_2$, and have dimensions $in_y \times j$ and $j \times j$, respectively. By doing so, one can write:

$$\bar{\boldsymbol{O}}_i = \boldsymbol{W}_1\boldsymbol{O}_i\boldsymbol{W}_2 \tag{75}$$

where $\bar{\boldsymbol{O}}_i$ identifies a matrix of dimensions $in_y \times j$ that represents the post-processed version of the fundamental matrix $\boldsymbol{O}_i$. Correctly choosing the weighting matrices $\boldsymbol{W}_1$ and $\boldsymbol{W}_2$ in the N4SID method is of fundamental importance for the successful implementation of the numerical procedure. In particular, three types of weighing matrices are used in this paper, namely the matrices that correspond to the Canonical Variate Analysis (CVA) technique, the matrices that correspond to the Multivariable Output-Error State sPace (MOESP) method, and the matrices that correspond to the Subspace State-space ARX (SSARX) approach. The weighting matrices of the first two methods are given in Table 1.

Table 1. Weighting matrices of the N4SID methods.

Method	Matrix $\boldsymbol{W}_1$	Matrix $\boldsymbol{W}_2$
CVA	$(\mathrm{E}[(\boldsymbol{Y}_f\boldsymbol{\Pi}_{\boldsymbol{U}_f^\perp})(\boldsymbol{Y}_f\boldsymbol{\Pi}_{\boldsymbol{U}_f^\perp})^T])^{-1/2}$	$\boldsymbol{\Pi}_{\boldsymbol{U}_f^\perp}$
MOESP	$\boldsymbol{I}$	$\boldsymbol{\Pi}_{\boldsymbol{U}_f^\perp}$

In Table 1, the mathematical symbol $\mathrm{E}[x]$ represents the expected value of the variable x. The weighting matrices $\boldsymbol{W}_1$ and $\boldsymbol{W}_2$ play the role of data filters. Therefore, the selection of these matrices has a significant impact on the quality of the numerical results produced by the identification process. On the other hand, by performing a Singular Value Decomposition (SVD) of the post-processed matrix $\bar{\boldsymbol{O}}_i$, one obtains:

$$\bar{\boldsymbol{O}}_i = \boldsymbol{U}\boldsymbol{\Sigma}\boldsymbol{V}^T \tag{76}$$

where $\boldsymbol{\Sigma}$ is a rectangular matrix of dimensions $in_y \times j$ that contains the singular values of the post-processed matrix $\bar{\boldsymbol{O}}_i$ resulting from the weighting process, whereas $\boldsymbol{U}$ and $\boldsymbol{V}$ are two square matrices arising from the numerical factorization having respectively dimensions $in_y \times in_y$ and $j \times j$. Consequently, the post-processed matrix $\bar{\boldsymbol{O}}_i$ can be partitioned as follows:

$$\bar{\boldsymbol{O}}_i = \boldsymbol{U}_1\boldsymbol{\Sigma}_1\boldsymbol{V}_1^T \tag{77}$$

where:

$$\boldsymbol{U} = \begin{bmatrix} \boldsymbol{U}_1 & \boldsymbol{U}_2 \end{bmatrix}, \quad \boldsymbol{\Sigma} = \begin{bmatrix} \boldsymbol{\Sigma}_1 & \boldsymbol{O} \\ \boldsymbol{O} & \boldsymbol{O} \end{bmatrix}, \quad \boldsymbol{V}^T = \begin{bmatrix} \boldsymbol{V}_1^T \\ \boldsymbol{V}_2^T \end{bmatrix} \tag{78}$$

where $\boldsymbol{U}_1$, $\boldsymbol{U}_2$, $\boldsymbol{V}_1$, and $\boldsymbol{V}_2$ are appropriate submatrices, which form the matrices $\boldsymbol{U}$ and $\boldsymbol{V}$ representing the factors of the singular value decomposition of the matrix $\bar{\boldsymbol{O}}_i$, having respectively dimensions $in_y \times \hat{n}_z$, $in_y \times (in_y - \hat{n}_z)$, $j \times \hat{n}_z$, and $j \times (j - \hat{n}_z)$. More importantly, the submatrix denoted with $\boldsymbol{\Sigma}_1$ is a square diagonal matrix of dimensions $\hat{n}_z \times \hat{n}_z$ given by:

$$\boldsymbol{\Sigma}_1 = \mathrm{diag}(\sigma_1, \sigma_2, ..., \sigma_{\hat{n}_z}) \tag{79}$$

where $\hat{n}_z$ is the number of the nonzero singular values denoted with $\sigma_h,\ h = 1, 2, ..., \hat{n}_z$, which identifies the principal dimension of the identified state-space model. Once the weighted matrix denoted with $\bar{\boldsymbol{O}}_i$ is identified through the use of the subspace algorithm described so far, the next fundamental process is the extraction of the state-space matrices from the identified spectrum of the mechanical system. To this end, one needs first to recover the matrix $\boldsymbol{O}_i$ as follows:

$$\boldsymbol{O}_i = \boldsymbol{W}_1^{-1}\boldsymbol{U}_1\boldsymbol{\Sigma}_1\boldsymbol{V}_1^T\boldsymbol{W}_2^{-1} \tag{80}$$

Considering Equation (74) in combination with Equation (80), one can write:

$$\boldsymbol{O}_i = \boldsymbol{W}_1^{-1}\boldsymbol{U}_1\boldsymbol{\Sigma}_1\boldsymbol{V}_1^T\boldsymbol{W}_2^{-1} = \boldsymbol{\Gamma}_i\boldsymbol{Z}_f \tag{81}$$

Equation (81) can be separated into two parts as follows:

$$\boldsymbol{\Gamma}_i = \boldsymbol{W}_1^{-1}\boldsymbol{U}_1\boldsymbol{\Sigma}_1^{1/2}\,\boldsymbol{T}, \quad \boldsymbol{Z}_f = \boldsymbol{T}^{-1}\boldsymbol{\Sigma}_1^{1/2}\,\boldsymbol{V}_1^T\boldsymbol{W}_2^{-1} \tag{82}$$

where $\boldsymbol{T}$ represents an appropriate non-singular square matrix of dimensions $\hat{n}_z \times \hat{n}_z$ representing a similarity transformation matrix, which can also be assumed as equal to the identity matrix to simplify the mathematical manipulations. By doing so, the matrices $\boldsymbol{\Gamma}_i$ and $\boldsymbol{Z}_f$ can be determined from Equation (82) as follows:

$$\boldsymbol{Z}_f = \boldsymbol{\Sigma}_1^{1/2}\,\boldsymbol{V}_1^T\boldsymbol{W}_2^{-1}, \quad \boldsymbol{\Gamma}_i = \boldsymbol{W}_1^{-1}\boldsymbol{U}_1\boldsymbol{\Sigma}_1^{1/2} \tag{83}$$

At this stage, the last step of the identification algorithm focuses on the computation of the discrete-time state-space matrices $\boldsymbol{A}_d$, $\boldsymbol{B}_d$, $\boldsymbol{C}_d$, and $\boldsymbol{D}_d$ based on the factorization process carried out before. For this purpose, the identified version of the discrete-time output influence matrix denoted with $\hat{\boldsymbol{C}}_d$ can be calculated directly by extracting the first n_y rows of the matrix $\boldsymbol{\Gamma}_i$ as:

$$\hat{\boldsymbol{C}}_d = \boldsymbol{E}_{n_y}^T\boldsymbol{\Gamma}_i \tag{84}$$

where $\boldsymbol{E}_{n_y}$ denotes an appropriate Boolean matrix useful for the matrix data extraction. Moreover, the identified version of the discrete-time state matrix denoted with $\hat{\boldsymbol{A}}_d$ can be constructed as follows:

$$\hat{\boldsymbol{A}}_d = (\underline{\boldsymbol{\Gamma}_i})^+\overline{\boldsymbol{\Gamma}_i} \tag{85}$$

where the matrix denoted with $(\underline{\boldsymbol{\Gamma}_i})^+$ represents the Moore-Penrose pseudoinverse of the matrix $\underline{\boldsymbol{\Gamma}_i}$, whereas $\underline{\boldsymbol{\Gamma}_i}$ identifies a modified version of the matrix $\boldsymbol{\Gamma}_i$ of dimensions $(i-1)n_y \times n_z$ in which the last matrix block of dimensions $n_y \times n_z$ is removed and $\overline{\boldsymbol{\Gamma}_i}$ identifies a modified version of the matrix $\boldsymbol{\Gamma}_i$ of dimensions $(i-1)n_y \times n_z$ in which the first matrix block of dimensions $n_y \times n_z$ is removed. These matrices are respectively defined as:

$$\underline{\boldsymbol{\Gamma}_i} = \begin{bmatrix} \boldsymbol{C}_d \\ \boldsymbol{C}_d\boldsymbol{A}_d \\ \boldsymbol{C}_d\boldsymbol{A}_d^2 \\ \vdots \\ \boldsymbol{C}_d\boldsymbol{A}_d^{i-2} \end{bmatrix}, \quad \overline{\boldsymbol{\Gamma}_i} = \begin{bmatrix} \boldsymbol{C}_d\boldsymbol{A}_d \\ \boldsymbol{C}_d\boldsymbol{A}_d^2 \\ \boldsymbol{C}_d\boldsymbol{A}_d^3 \\ \vdots \\ \boldsymbol{C}_d\boldsymbol{A}_d^{i-1} \end{bmatrix} \tag{86}$$

By multiplying Equation (55) by $\boldsymbol{U}_f^+$ and $\boldsymbol{\Gamma}_i^\perp$, the identified version of the input influence matrix denoted with $\hat{\boldsymbol{B}}_d$ and of the direct transmission matrix denoted with $\hat{\boldsymbol{D}}$ can be extracted. To this end, one can write:

$$\boldsymbol{\Gamma}_i^\perp \boldsymbol{Y}_f \boldsymbol{U}_f^+ = \boldsymbol{\Gamma}_i^\perp \boldsymbol{\Gamma}_i \boldsymbol{Z}_f \boldsymbol{U}_f^+ + \boldsymbol{\Gamma}_i^\perp \boldsymbol{H}_i \boldsymbol{U}_f \boldsymbol{U}_f^+ = \boldsymbol{\Gamma}_i^\perp \boldsymbol{H}_i \tag{87}$$

where the matrix $\boldsymbol{U}_f^+$ represents the Moore-Penrose pseudoinverse of the matrix $\boldsymbol{U}_f$, whereas $\boldsymbol{\Gamma}_i^\perp$ is a full rank matrix representing the projection matrix associated with the observability matrix $\boldsymbol{\Gamma}_i$. Furthermore, to simplify the notation, one can introduce the following matrices:

$$\boldsymbol{N} = \boldsymbol{\Gamma}_i^\perp \boldsymbol{Y}_f \boldsymbol{U}_f^+, \quad \boldsymbol{P} = \boldsymbol{\Gamma}_i^\perp \tag{88}$$

where $\boldsymbol{N}$ and $\boldsymbol{P}$ are rectangular matrices having dimensions $n_z \times in_u$ and $n_z \times in_y$, respectively. By doing so, Equation (87) can then be rewritten as follows:

$$\boldsymbol{N} = \boldsymbol{P}\boldsymbol{H}_i \tag{89}$$

Subsequently, Equation (89) can be expanded in the following matrix form:

$$\begin{bmatrix} \boldsymbol{N}_1 & \boldsymbol{N}_2 & \dots & \boldsymbol{N}_i \end{bmatrix} = \begin{bmatrix} \boldsymbol{P}_1 & \boldsymbol{P}_2 & \dots & \boldsymbol{P}_i \end{bmatrix} \boldsymbol{H}_i \tag{90}$$

Equation (90) leads to:

$$\begin{bmatrix} \boldsymbol{N}_1 \\ \boldsymbol{N}_2 \\ \vdots \\ \boldsymbol{N}_i \end{bmatrix} = \begin{bmatrix} \boldsymbol{P}_1 & \boldsymbol{P}_2 & \dots & \boldsymbol{P}_i \\ \boldsymbol{P}_2 & \boldsymbol{P}_3 & \dots & \boldsymbol{O} \\ \vdots & \vdots & \ddots & \vdots \\ \boldsymbol{P}_i & \boldsymbol{O} & \dots & \boldsymbol{O} \end{bmatrix} \begin{bmatrix} \boldsymbol{I} & \boldsymbol{O} \\ \boldsymbol{O} & \underline{\boldsymbol{\Gamma}_i} \end{bmatrix} \boldsymbol{\Omega} \tag{91}$$

where $\boldsymbol{\Omega}$ is a rectangular matrix of dimensions $(n_z + n_y) \times n_u$ defined as:

$$\boldsymbol{\Omega} = \begin{bmatrix} \boldsymbol{D}_d \\ \boldsymbol{B}_d \end{bmatrix} \tag{92}$$

It finally follows that:

$$\boldsymbol{\Omega} = \begin{bmatrix} \boldsymbol{I} & \boldsymbol{O} \\ \boldsymbol{O} & \underline{\boldsymbol{\Gamma}_i} \end{bmatrix}^+ \begin{bmatrix} \boldsymbol{P}_1 & \boldsymbol{P}_2 & \dots & \boldsymbol{P}_i \\ \boldsymbol{P}_2 & \boldsymbol{P}_3 & \dots & \boldsymbol{O} \\ \vdots & \vdots & \ddots & \vdots \\ \boldsymbol{P}_i & \boldsymbol{O} & \dots & \boldsymbol{O} \end{bmatrix}^+ \begin{bmatrix} \boldsymbol{N}_1 \\ \boldsymbol{N}_2 \\ \vdots \\ \boldsymbol{N}_i \end{bmatrix} \tag{93}$$

Once the matrix $\boldsymbol{\Omega}$ is numerically determined, the identified version of the matrices $\boldsymbol{B}_d$ and $\boldsymbol{D}_d$ can be readily extracted. For this purpose, one can write:

$$\hat{\boldsymbol{D}}_d = \boldsymbol{E}_{n_y}^T \boldsymbol{\Omega}, \quad \hat{\boldsymbol{B}}_d = \boldsymbol{E}_{n_z}^T \boldsymbol{\Omega} \tag{94}$$

where $\boldsymbol{E}_{n_y}$ and $\boldsymbol{E}_{n_z}$ represent appropriate Boolean matrices, which respectively serve for recovering the identified discrete-time direct transmission matrix $\hat{\boldsymbol{D}}_d$ and the identified discrete-time input influence matrix $\hat{\boldsymbol{B}}_d$ from the first n_y rows and the last n_z rows of the matrix $\boldsymbol{\Omega}$. In synthesis, the identified version of the discrete-time state-space matrices of the mechanical system can be explicitly calculated using the N4SID method as follows:

$$\begin{cases} \hat{\boldsymbol{A}}_d = \left(\underline{\boldsymbol{\Gamma}_i}\right)^+ \overline{\boldsymbol{\Gamma}_i} \\ \hat{\boldsymbol{B}}_d = \boldsymbol{E}_{n_z}^T \boldsymbol{\Omega} \\ \hat{\boldsymbol{C}}_d = \boldsymbol{E}_{n_y}^T \boldsymbol{\Gamma}_i \\ \hat{\boldsymbol{D}}_d = \boldsymbol{E}_{n_y}^T \boldsymbol{\Omega} \end{cases} \tag{95}$$

where $\hat{\boldsymbol{A}}_d$ is the identified discrete-time state matrix, $\hat{\boldsymbol{B}}_d$ is the identified discrete-time input influence matrix, $\hat{\boldsymbol{C}}_d$ is the identified discrete-time output influence matrix, and $\hat{\boldsymbol{D}}_d$ is the identified discrete-time direct transmission matrix.

3.3 Identification of the Mass, Stiffness, and Damping Matrices (MKR)

In this subsection, the fundamental steps of a general method for constructing second-order configuration-space mechanical models of a given dynamical system starting from its first-order state-space realizations obtained using the identification algorithms described before are revised [31,32]. In general, a physical model of a linear mechanical system is completely described by the triplet of matrices containing the mass matrix denoted with $\boldsymbol{M}$, the stiffness matrix denoted with $\boldsymbol{K}$, and the damping matrix denoted with $\boldsymbol{R}$. In the continuous-time domain, the second-order physical model of a mechanical system can be readily converted into a first-order state-space model, which is represented by the quartet of matrices containing the state matrix denoted with $\boldsymbol{A}_c$, the input influence matrix denoted with $\boldsymbol{B}_c$, the output influence matrix denoted with $\boldsymbol{C}_c$, and the direct transmission matrix denoted with $\boldsymbol{D}_c$. This problem is sometimes referred to as the forward linear vibration problem. On the other hand, the inverse problem is more complex since there are several algorithms that allow for experimentally determining a first-order state-space model from input and output measurements. To this end, a proper triplet of mass, stiffness, and damping matrices, respectively denoted with $\hat{\boldsymbol{M}}$, $\hat{\boldsymbol{K}}$, and $\hat{\boldsymbol{R}}$, can be recovered from the continuous-time matrices, which are formed by the identified state matrix $\hat{\boldsymbol{A}}_c$ and the identified input influence matrix $\hat{\boldsymbol{B}}_c$, as well as the identified output influence matrix $\hat{\boldsymbol{C}}_c$ and the identified direct transmission matrix $\hat{\boldsymbol{D}}_c$. Since this method represents a solution for the general problem known as the inverse linear vibration problem, that is, how to properly find the mass, stiffness, and damping matrices that physically describe the input-output dataset measured for a given mechanical system to be identified, the numerical procedure for computing these matrices of interest is herein referred to as the MKR method.

The physically consistent transformation of an identified state-space model into an identified configuration-space model is not a straightforward task, and it can be carried out by employing different methods, depending on the state-space coordinates chosen to represent the system as well as the actual location on the physical system of the actuators and sensors used for recording the input-output data. In particular, for effectively implementing the MKR method introduced here, the basic requirement is that all system degrees of freedom must be instrumented with a sensor or an actuator, with at least one co-located actuator-sensor pair. For this purpose, consider the following alternative representation of the continuous-time state-space model of a general dynamical system:

$$\begin{cases} \boldsymbol{R}\dot{\boldsymbol{z}}_1 + \boldsymbol{M}\dot{\boldsymbol{z}}_2 = -\boldsymbol{K}\boldsymbol{z}_1 + \boldsymbol{B}_a\boldsymbol{u} \\ \boldsymbol{M}\dot{\boldsymbol{z}}_1 = \boldsymbol{M}\boldsymbol{z}_2 \end{cases} \tag{96}$$

which can be written in the following compact matrix form:

$$\boldsymbol{U}_c\dot{\boldsymbol{z}} = \boldsymbol{V}_c\boldsymbol{z} + \boldsymbol{E}_c\boldsymbol{u} \tag{97}$$

where $\boldsymbol{U}_c$ is a square symmetric matrix of dimensions $n_z \times n_z$ representing the system transition matrix associated with the time derivative of the state vector, $\boldsymbol{V}_c$ is a square symmetric matrix of dimensions $n_z \times n_z$ representing the system transition matrix associated with the state vector, and $\boldsymbol{E}_c$ is a rectangular matrix of dimensions $n_z \times n_u$ representing the system transition matrix associated with the input vector. These matrices are respectively defined as follows:

$$\boldsymbol{U}_c = \begin{bmatrix} \boldsymbol{R} & \boldsymbol{M} \\ \boldsymbol{M} & \boldsymbol{O} \end{bmatrix}, \quad \boldsymbol{V}_c = \begin{bmatrix} -\boldsymbol{K} & \boldsymbol{O} \\ \boldsymbol{O} & \boldsymbol{M} \end{bmatrix}, \quad \boldsymbol{E}_c = \begin{bmatrix} \boldsymbol{B}_a \\ \boldsymbol{O} \end{bmatrix} \tag{98}$$

where $\boldsymbol{O}$ denotes a zero matrix having proper dimensions. It is important to note that the alternative state-space formulation proposed here and described in Equation (97) is general and versatile. In fact, this formulation includes as a special case the scenario in which the transition matrix $\boldsymbol{U}_c$ is nonsingular and, therefore, it can be numerically inverted. This special case leads to the conventional continuous-time state-space model given by Equation (5), where the system state matrix is given by $\boldsymbol{A}_c = \boldsymbol{U}_c^{-1}\boldsymbol{V}_c$ and the system input influence matrix is given by $\boldsymbol{B}_c = \boldsymbol{U}_c^{-1}\boldsymbol{E}_c$. The peculiarity of this alternative continuous-time state-space representation is that the associated eigenvalue problem turns out to be symmetric as well. Therefore, this problem can be conveniently written in a matrix form as follows:

$$\boldsymbol{V}_c\boldsymbol{\Psi}_c = \boldsymbol{U}_c\boldsymbol{\Psi}_c\boldsymbol{\Lambda}_c \tag{99}$$

where $\boldsymbol{\Lambda}_c$ is a square diagonal matrix of dimensions $n_z \times n_z$ containing the eigenvalues of the system continuous-time state-space model and $\boldsymbol{\Psi}_c$ is a square matrix of dimensions $n_z \times n_z$ containing the system eigenvectors grouped by column.

Exploiting the general state-space formulation introduced herein and the resulting diagonal form of the eigenvalue matrix denoted with $\boldsymbol{\Lambda}_c$, the eigenvector matrix denoted with $\boldsymbol{\Psi}_c$ can be conveniently partitioned in the following matrix form:

$$\boldsymbol{\Psi}_c = \begin{bmatrix} \boldsymbol{W}_c \\ \boldsymbol{W}_c\boldsymbol{\Lambda}_c \end{bmatrix} \tag{100}$$

where $\boldsymbol{W}_c$ is a rectangular matrix having dimensions $n_x \times n_z$ that identifies the eigenvector matrix associated to the system configuration-space physical coordinates, while the square matrix $\boldsymbol{\Psi}_c$ of dimensions $n_z \times n_z$ represents the eigenvector matrix relative to the system state-space mathematical coordinates. In particular, the eigenvector matrix $\boldsymbol{W}_c$ of dimensions $n_x \times n_z$ is, in turn, related to the eigenvector matrix $\boldsymbol{\Phi}_c$ of dimensions $n_x \times n_x$ by the following relationship:

$$\boldsymbol{W}_c = \begin{bmatrix} \boldsymbol{\varphi}_{c,1} & \boldsymbol{\varphi}^*_{c,1} & \boldsymbol{\varphi}_{c,2} & \boldsymbol{\varphi}^*_{c,2} & \cdots & \boldsymbol{\varphi}_{c,n_x} & \boldsymbol{\varphi}^*_{c,n_x} \end{bmatrix} \tag{101}$$

where:

$$\boldsymbol{\Phi}_c = \begin{bmatrix} \boldsymbol{\varphi}_{c,1} & \boldsymbol{\varphi}_{c,2} & \cdots & \boldsymbol{\varphi}_{c,n_x} \end{bmatrix} \tag{102}$$

where the generic vector $\boldsymbol{\varphi}_{c,j},\ j = 1, 2, \ldots, n_x$ of dimensions $n_x \times 1$ indicates the generic eigenvector of the second-order configuration-space model and the generic vector $\boldsymbol{\varphi}^*_{c,j},\ j = 1, 2, \ldots, n_x$ indicates its complex conjugate. Considering a structural vibration problem, one can reasonably assume that all the normal modes of the dynamical model of the underlying mechanical system are underdamped. Therefore, the eigenvalues are supposed to appear in complex conjugate pairs, and the system continuous-time eigenvalue matrix $\boldsymbol{\Lambda}_c$ can be written as follows:

$$\boldsymbol{\Lambda}_c = \mathrm{diag}(\lambda_{c,1}, \lambda_{c,2}, \ldots, \lambda_{c,n_z-1}, \lambda_{c,n_z}) \tag{103}$$

where:

$$\lambda_{c,j} = a_{c,j} \pm i b_{c,j} = -\xi_j\omega_{n,j} \pm i\sqrt{1-\xi_j^2}\,\omega_{n,j}, \quad j = 1, 2, \ldots, n_x \tag{104}$$

where $i = \sqrt{-1}$ is the imaginary unit, $\lambda_{c,j},\ j = 1, 2, \ldots, n_x$ are the continuous-time state-space eigenvalues, $a_{c,j},\ j = 1, 2, \ldots, n_x$ and $b_{c,j},\ j = 1, 2, \ldots, n_x$ respectively represent the real and imaginary parts of the system eigenvalues, whereas $\omega_{n,j},\ j = 1, 2, \ldots, n_x$ and $\xi_j,\ j = 1, 2, \ldots, n_x$ respectively indicate the system natural angular frequencies and the system dimensionless damping ratios.

Since, in principle, the scaling of the eigenvectors is fundamentally arbitrary, one can conveniently assume that the columns of the eigenvector matrix denoted with $\boldsymbol{\Psi}_c$ are scaled such that the following two equations hold:

$$\boldsymbol{\Psi}_c^T\boldsymbol{U}_c\boldsymbol{\Psi}_c = \boldsymbol{I} \quad \Leftrightarrow \quad \begin{bmatrix} \boldsymbol{W}_c \\ \boldsymbol{W}_c\boldsymbol{\Lambda}_c \end{bmatrix}^T \begin{bmatrix} \boldsymbol{R} & \boldsymbol{M} \\ \boldsymbol{M} & \boldsymbol{O} \end{bmatrix} \begin{bmatrix} \boldsymbol{W}_c \\ \boldsymbol{W}_c\boldsymbol{\Lambda}_c \end{bmatrix} = \boldsymbol{I} \tag{105}$$

and

$$\boldsymbol{\Psi}_c^T\boldsymbol{V}_c\boldsymbol{\Psi}_c = \boldsymbol{\Lambda}_c \quad \Leftrightarrow \quad \begin{bmatrix} \boldsymbol{W}_c \\ \boldsymbol{W}_c\boldsymbol{\Lambda}_c \end{bmatrix}^T \begin{bmatrix} -\boldsymbol{K} & \boldsymbol{O} \\ \boldsymbol{O} & \boldsymbol{M} \end{bmatrix} \begin{bmatrix} \boldsymbol{W}_c \\ \boldsymbol{W}_c\boldsymbol{\Lambda}_c \end{bmatrix} = \boldsymbol{\Lambda}_c \tag{106}$$

where $\boldsymbol{I}$ denotes an identity matrix having proper dimensions. These equations respectively lead to:

$$\boldsymbol{W}_c^T\boldsymbol{R}\boldsymbol{W}_c + \boldsymbol{W}_c^T\boldsymbol{M}\boldsymbol{W}_c\boldsymbol{\Lambda}_c + \boldsymbol{\Lambda}_c^T\boldsymbol{W}_c^T\boldsymbol{M}\boldsymbol{W}_c = \boldsymbol{I} \tag{107}$$

and

$$-\boldsymbol{W}_c^T\boldsymbol{K}\boldsymbol{W}_c + \boldsymbol{\Lambda}_c^T\boldsymbol{W}_c^T\boldsymbol{M}\boldsymbol{W}_c\boldsymbol{\Lambda}_c = \boldsymbol{\Lambda}_c \tag{108}$$

The assumptions leading to Equations (105) and (106) represent a key feature of the MKR method, whose fundamental consequences are twofold. The first immediate consequence is that the modal representation of the continuous-time state-space model assumes the following particular form:

$$\begin{cases} \dot{\boldsymbol{z}}_m = \boldsymbol{A}_{c,m}\boldsymbol{z}_m + \boldsymbol{B}_{c,m}\boldsymbol{u} \\ \boldsymbol{y} = \boldsymbol{C}_{c,m}\boldsymbol{z}_m + \boldsymbol{D}_{c,m}\boldsymbol{u} \end{cases} \tag{109}$$

where $\boldsymbol{z}_m$ is a vector having dimensions $n_z \times 1$ representing the modal state vector, whereas the matrices $\boldsymbol{A}_{c,m}$, $\boldsymbol{B}_{c,m}$, $\boldsymbol{C}_{c,m}$, and $\boldsymbol{D}_{c,m}$ respectively represent the continuous-time modal state matrix of dimensions $n_z \times n_z$, the continuous-time modal input influence matrix of dimensions $n_z \times n_u$, the continuous-time modal output influence matrix of dimensions $n_y \times n_z$, and the continuous-time modal direct transmission matrix of dimensions $n_y \times n_u$. One can easily prove that these state-space modal matrices can be respectively computed as follows:

$$\boldsymbol{A}_{c,m} = \boldsymbol{\Lambda}_c, \quad \boldsymbol{B}_{c,m} = \boldsymbol{W}_c^T\boldsymbol{B}_a, \quad \boldsymbol{C}_{c,m} = \boldsymbol{C}_s\boldsymbol{W}_c\boldsymbol{\Lambda}_c^b, \quad \boldsymbol{D}_{c,m} = \boldsymbol{D}_c \tag{110}$$

where $\boldsymbol{C}_s$ is a rectangular matrix of dimensions $n_y \times n_z$ and b is a scalar integer associated to the type of sensing equipment. More specifically, for displacement sensing, one has $\boldsymbol{C}_s = \boldsymbol{C}_p$ and $b = 0$; for velocity sensing, one has $\boldsymbol{C}_s = \boldsymbol{C}_v$ and $b = 1$; for acceleration sensing, one has $\boldsymbol{C}_s = \boldsymbol{C}_a$ and $b = 2$; where $\boldsymbol{C}_p$, $\boldsymbol{C}_v$, and $\boldsymbol{C}_a$ respectively represent rectangular matrices of dimensions $n_y \times n_z$ associated to the displacement, velocity, and acceleration sensing that characterize the configuration-space measurement equations introduced in Equation (7).

As shown in Equation (110), it is worth noting that the modal input influence matrix $\boldsymbol{B}_{c,m}$ is determined by using the transpose of the configuration-space eigenvector matrix $\boldsymbol{W}_c$ instead of using the inverse of the state-space eigenvector matrix $\boldsymbol{\Psi}_c$, whereas the direct transmission matrix $\boldsymbol{D}_{c,m}$ is unaffected by the modal transformation. As mentioned before, the eigenvector scaling used in the MKR method and described by Equations (105) and (106) have two fundamental consequences. The second consequence of the selected scaling hypothesis used for the system state-space eigenvectors is that the mass, stiffness, and damping matrices describing the system configuration-space model can be directly extracted from the state-space eigenvalue matrix $\boldsymbol{\Lambda}_c$ and the configuration-space eigenvector matrix $\boldsymbol{W}_c$. To achieve this goal, the orthogonality conditions given by Equations (105) and (106) can be reformulated as follows:

$$\boldsymbol{U}_c^{-1} = \boldsymbol{\Psi}_c\boldsymbol{\Psi}_c^T, \quad \boldsymbol{V}_c^{-1} = \boldsymbol{\Psi}_c\boldsymbol{\Lambda}_c^{-1}\boldsymbol{\Psi}_c^T \tag{111}$$

which leads to the following matrix equations:

$$\begin{bmatrix} \boldsymbol{O} & \boldsymbol{M}^{-1} \\ \boldsymbol{M}^{-1} & -\boldsymbol{M}^{-1}\boldsymbol{R}\boldsymbol{M}^{-1} \end{bmatrix} = \begin{bmatrix} \boldsymbol{W}_c\boldsymbol{W}_c^T & \boldsymbol{W}_c\boldsymbol{\Lambda}_c^T\boldsymbol{W}_c^T \\ \boldsymbol{W}_c\boldsymbol{\Lambda}_c\boldsymbol{W}_c^T & \boldsymbol{W}_c\boldsymbol{\Lambda}_c^2\boldsymbol{W}_c^T \end{bmatrix} \tag{112}$$

and

$$\begin{bmatrix} -\boldsymbol{K}^{-1} & \boldsymbol{O} \\ \boldsymbol{O} & \boldsymbol{M}^{-1} \end{bmatrix} = \begin{bmatrix} \boldsymbol{W}_c\boldsymbol{\Lambda}_c^{-1}\boldsymbol{W}_c^T & \boldsymbol{W}_c\boldsymbol{W}_c^T \\ \boldsymbol{W}_c\boldsymbol{W}_c^T & \boldsymbol{W}_c\boldsymbol{\Lambda}_c\boldsymbol{W}_c^T \end{bmatrix} \tag{113}$$

Consequently, one can directly recognize the following two sets of identities:

$$\boldsymbol{M}^{-1} = \boldsymbol{W}_c\boldsymbol{\Lambda}_c^T\boldsymbol{W}_c^T, \quad -\boldsymbol{M}^{-1}\boldsymbol{R}\boldsymbol{M}^{-1} = \boldsymbol{W}_c\boldsymbol{\Lambda}_c^2\boldsymbol{W}_c^T \tag{114}$$

and

$$-\boldsymbol{K}^{-1} = \boldsymbol{W}_c\boldsymbol{\Lambda}_c^{-1}\boldsymbol{W}_c^T, \quad \boldsymbol{W}_c\boldsymbol{W}_c^T = \boldsymbol{O} \tag{115}$$

By doing so, it can be easily demonstrated that the matrices $\boldsymbol{M}$, $\boldsymbol{K}$, and $\boldsymbol{R}$ describing the second-order model of the mechanical system of interest can be constructed by adopting the fundamental equations of the MKR method as follows:

$$\begin{cases} \boldsymbol{M} = \left(\boldsymbol{W}_c\boldsymbol{\Lambda}_c\boldsymbol{W}_c^T\right)^{-1} \\ \boldsymbol{K} = -\left(\boldsymbol{W}_c\boldsymbol{\Lambda}_c^{-1}\boldsymbol{W}_c^T\right)^{-1} \\ \boldsymbol{R} = -\boldsymbol{M}\boldsymbol{W}_c\boldsymbol{\Lambda}_c^2\boldsymbol{W}_c^T\boldsymbol{M} \end{cases} \tag{116}$$

Equation (116) contains the key relations that characterize the MKR method. At this stage, the fundamental problem of the present identification procedure is the proper reconstruction of the configuration-space eigenvector matrix $\boldsymbol{W}_c$ from the system modal continuous-time state-space model, characterized by the state-space eigenvalue matrix $\boldsymbol{\Lambda}_c$ and the state-space eigenvector matrix $\boldsymbol{\Psi}_c$, namely how to extract an identified version of the configuration-space eigenvector matrix $\hat{\boldsymbol{W}}_c$ from an identified state-space representation defined by the identified set of matrices $\hat{\boldsymbol{A}}_c$, $\hat{\boldsymbol{B}}_c$, $\hat{\boldsymbol{C}}_c$, and $\hat{\boldsymbol{D}}_c$.

Since the modal parameters of a given dynamical system must be the same regardless of the type of state-space formulation used, the problem of finding the configuration-space eigenvector matrix $\boldsymbol{W}_c$ reduces to the problem of determining a proper transformation of coordinates. Thus, one needs to find a suitable transformation matrix denoted with $\boldsymbol{T}$ capable of converting the identified set of modal parameters, arising from a general system state-space formulation that is characterized by the quartet of modal matrices given by $\hat{\boldsymbol{A}}_{c,m} = \hat{\boldsymbol{\Lambda}}_c$, $\hat{\boldsymbol{B}}_{c,m} = \hat{\boldsymbol{\Psi}}_c^{-1}\hat{\boldsymbol{B}}_c$, $\hat{\boldsymbol{C}}_{c,m} = \hat{\boldsymbol{C}}_c\hat{\boldsymbol{\Psi}}_c$, and $\hat{\boldsymbol{D}}_{c,m} = \hat{\boldsymbol{D}}_c$, into a special set of modal parameters, generated by the symmetric system state-space formulation that is defined by the quartet of modal matrices given by $\boldsymbol{A}_{c,m} = \boldsymbol{\Lambda}_c$, $\boldsymbol{B}_{c,m} = \boldsymbol{W}_c^T\boldsymbol{B}_a$, $\boldsymbol{C}_{c,m} = \boldsymbol{C}_s\boldsymbol{W}_c\boldsymbol{\Lambda}_c^b$, and $\boldsymbol{D}_{c,m} = \boldsymbol{D}_c$. To achieve the desired goal, the corresponding coordinate transformation problem can be mathematically stated in the following matrix form:

$$\boldsymbol{T}^{-1}\hat{\boldsymbol{\Lambda}}_c\boldsymbol{T} = \boldsymbol{\Lambda}_c, \quad \boldsymbol{T}^{-1}\hat{\boldsymbol{\Psi}}_c^{-1}\hat{\boldsymbol{B}}_c = \boldsymbol{W}_c^T\boldsymbol{B}_a \tag{117}$$

and

$$\hat{\boldsymbol{C}}_c\hat{\boldsymbol{\Psi}}_c\boldsymbol{T} = \boldsymbol{C}_s\boldsymbol{W}_c\boldsymbol{\Lambda}_c^b, \quad \hat{\boldsymbol{D}}_c = \boldsymbol{D}_c \tag{118}$$

where $\boldsymbol{T}$ represents an appropriate transformation matrix having dimensions $n_z \times n_z$. Since the eigenvalues are equal in both the state-space representations, one can deduce that the transformation matrix $\boldsymbol{T}$ of interest must be a diagonal matrix composed of complex conjugate elements. Moreover, the desired transformation matrix $\boldsymbol{T}$ must produce two fundamental effects, which are the transformation of the eigenvectors from those of an asymmetric eigenvalue problem into those of a symmetric problem and the proper scaling of such eigenvectors. Another important observation that serves for the determination of the transformation matrix $\boldsymbol{T}$ is that, in virtue of the initial fundamental hypothesis concerning the measurement system, the mechanical system must feature at least one set of co-located actuators and sensors. Thus, this basic assumption implies the following matrix equation:

$$(\boldsymbol{C}_s)_{r=i}\boldsymbol{W}_c = \left(\boldsymbol{W}_c^T(\boldsymbol{B}_a)_{c=i}\right)^T \tag{119}$$

where $(\boldsymbol{C}_s)_{r=i}$ indicates the i row of the matrix $\boldsymbol{C}_s$ and $(\boldsymbol{B}_a)_{c=i}$ indicates the i column of the matrix $\boldsymbol{B}_a$. Note that Equation (119) simply holds because the rectangular matrices $\boldsymbol{C}_s$ and $\boldsymbol{B}_a$ are Boolean matrices composed of zeros and ones. By exploiting Equation (119), arising from the assumption of the existence of at least one set of co-located actuator-sensor pairs, together with Equations (117) and (118), deriving from the proper scaling of the system eigenvectors as well as the fundamental properties of the modal spectrum, one can show that the desired transformation matrix denoted with $\boldsymbol{T}$ can be calculated by using the identified realization of the system dynamic model and the identified modal parameters as follows:

$$\left(\hat{\boldsymbol{C}}_c^E\right)_{r=i}\hat{\boldsymbol{\Psi}}_c\hat{\boldsymbol{\Lambda}}_c^{-b}\boldsymbol{T}^2 = \left(\hat{\boldsymbol{\Psi}}_c^{-1}\left(\hat{\boldsymbol{B}}_c^E\right)_{c=i}\right)^T \tag{120}$$

where $\hat{\boldsymbol{B}}_c^E$ and $\hat{\boldsymbol{C}}_c^E$ are square matrices of dimensions $n_z \times n_z$ respectively representing the expanded version of the identified input influence matrix denoted with $\hat{\boldsymbol{B}}_c$ and the expanded version of the identified output influence matrix denoted with $\hat{\boldsymbol{C}}_c$ that properly include additional rows and columns of zeros in order to match the dimension n_z, whereas $\left(\hat{\boldsymbol{C}}_c^E\right)_{r=i}$ indicates the i row of the matrix $\hat{\boldsymbol{C}}_c^E$, and $\left(\hat{\boldsymbol{B}}_c^E\right)_{c=i}$ indicates the i column of the matrix $\hat{\boldsymbol{B}}_c^E$. Since the transformation matrix $\boldsymbol{T}$ is a square diagonal matrix, its elements can be easily determined through the use of Equation (120). Once the transformation matrix $\boldsymbol{T}$ is known, the rows of the eigenvector matrix $\boldsymbol{\Phi}_c$ can be identified from each degree of freedom which is instrumented with a sensor or with an actuator. To this end, one can write:

$$(\boldsymbol{\Phi}_c)_{r=j} = \left(\boldsymbol{T}^{-1}\hat{\boldsymbol{\Psi}}_c^{-1}\left(\hat{\boldsymbol{B}}_c^E\right)_{c=j}\right)^T \tag{121}$$

and

$$(\boldsymbol{\Phi}_c)_{r=k} = \left(\hat{\boldsymbol{C}}_c^E\right)_{r=k}\hat{\boldsymbol{\Psi}}_c\hat{\boldsymbol{\Lambda}}_c^{-b}\boldsymbol{T} \tag{122}$$

where j identifies a generic degree of freedom instrumented with an actuator, k identifies a generic degree of freedom instrumented with a sensor, $(\boldsymbol{\Phi}_c)_{r=j}$ indicates the j row of the matrix $\boldsymbol{\Phi}_c$, $(\boldsymbol{\Phi}_c)_{r=k}$ indicates the k row of the matrix $\boldsymbol{\Phi}_c$, $\left(\hat{\boldsymbol{C}}_c^E\right)_{r=j}$ indicates the j row of the matrix $\hat{\boldsymbol{C}}_c^E$ and $\left(\hat{\boldsymbol{B}}_c^E\right)_{c=k}$ indicates the k column of the matrix $\hat{\boldsymbol{B}}_c^E$.

Finally, using the identified eigenvector matrix $\hat{\boldsymbol{W}}_c$ in conjunction with the identified eigenvalue matrix $\hat{\boldsymbol{\Lambda}}_c$, a second-order model of the mechanical system under study can be constructed by using the following procedure representing the MKR method:

$$\begin{cases} \hat{\boldsymbol{M}} = \left(\hat{\boldsymbol{W}}_c\hat{\boldsymbol{\Lambda}}_c\hat{\boldsymbol{W}}_c^T\right)^{-1} \\ \hat{\boldsymbol{K}} = -\left(\hat{\boldsymbol{W}}_c\hat{\boldsymbol{\Lambda}}_c^{-1}\hat{\boldsymbol{W}}_c^T\right)^{-1} \\ \hat{\boldsymbol{R}} = -\hat{\boldsymbol{M}}\hat{\boldsymbol{W}}_c\hat{\boldsymbol{\Lambda}}_c^2\hat{\boldsymbol{W}}_c^T\hat{\boldsymbol{M}} \end{cases} \tag{123}$$

where $\hat{\boldsymbol{M}}$ represents the identified mass matrix, $\hat{\boldsymbol{K}}$ represents the identified stiffness matrix, and $\hat{\boldsymbol{R}}$ represents the identified damping matrix. As a final remark, the identified damping matrix denoted with $\hat{\boldsymbol{R}}$ is hard to correctly estimate, and, therefore, the use of a separate algorithm for improving the estimation of the damping matrix is advocated.

3.4 Identification of the Proportional Damping Coefficients (PDC)

In this subsection, an effective least-square strategy for calculating an estimation of the proportional damping coefficients is presented, which leads to an improvement in the identification of the system damping matrix [43, 44]. For this purpose, the Proportional Damping Coefficients identification method (PDC) is presented herein. As discussed before, the mass, spring, and damping matrices of the mechanical system of interest can be readily obtained by the MKR method. However, as demonstrated by the implementation and the use of this method in practical applications, the damping matrix is significantly affected by the noise that corrupts the input and output measurements. Therefore, the PDC method can be used to improve the identification of the damping matrix with the use of a simple least-squares estimation procedure. To this end, the hypothesis of proportional damping is assumed, since this assumption can be considered acceptable in the case of lightly damped structural systems. By doing so, in the PDC method, the damping matrix is expressed in terms of the mass and stiffness matrices through the use of two proportional coefficients. Under these conditions, one can write:

$$\boldsymbol{R} = \alpha\boldsymbol{M} + \beta\boldsymbol{K} \tag{124}$$

where α and β denote the mass and stiffness proportional coefficients, respectively. The hypothesis of proportional damping directly implies the following set of equations:

$$\xi_i = \frac{\alpha}{2\omega_{n,i}} + \frac{\beta\omega_{n,i}}{2}, \quad i = 1, 2, \ldots, n_z \tag{125}$$

where $\omega_{n,i},\ i = 1, 2, \ldots, n_z$ represent the set of the system natural angular frequencies, while $\xi_{,i},\ i = 1, 2, \ldots, n_z$ represent the set of the system damping ratios. The goal of the PDC method is, therefore, to identify an appropriate couple of proportional coefficients denoted with $\hat{\alpha}$ and $\hat{\beta}$ for improving the estimation of the damping matrix $\hat{\boldsymbol{R}}$. In particular, in the PDC method, the coefficients $\hat{\alpha}$ and $\hat{\beta}$ are estimated from identified natural angular frequencies and the identified damping ratios by employing the following least-square computational approach:

$$\begin{cases} \frac{1}{2\hat{\omega}_{n,1}}\hat{\alpha} + \frac{\hat{\omega}_{n,1}}{2}\hat{\beta} = \hat{\xi}_1 \\ \frac{1}{2\hat{\omega}_{n,2}}\hat{\alpha} + \frac{\hat{\omega}_{n,2}}{2}\hat{\beta} = \hat{\xi}_2 \\ \vdots \\ \frac{1}{2\hat{\omega}_{n,\hat{n}_z}}\hat{\alpha} + \frac{\hat{\omega}_{n,\hat{n}_z}}{2}\hat{\beta} = \hat{\xi}_{\hat{n}_z} \end{cases} \tag{126}$$

Equation (126) can readily expressed in matrix form as follows:

$$\begin{bmatrix} \frac{1}{2\hat{\omega}_{n,1}} & \frac{\hat{\omega}_{n,1}}{2} \\ \frac{1}{2\hat{\omega}_{n,2}} & \frac{\hat{\omega}_{n,2}}{2} \\ \vdots & \vdots \\ \frac{1}{2\hat{\omega}_{n,\hat{n}_z}} & \frac{\hat{\omega}_{n,\hat{n}_z}}{2} \end{bmatrix} \begin{bmatrix} \hat{\alpha} \\ \hat{\beta} \end{bmatrix} = \begin{bmatrix} \hat{\xi}_1 \\ \hat{\xi}_2 \\ \vdots \\ \hat{\xi}_{\hat{n}_z} \end{bmatrix} \tag{127}$$

which leads to:

$$\bar{\boldsymbol{C}}_\omega \bar{\boldsymbol{x}} = \bar{\boldsymbol{d}}_\xi \quad \Rightarrow \quad \bar{\boldsymbol{x}} = \bar{\boldsymbol{C}}_\omega^+ \bar{\boldsymbol{d}}_\xi \tag{128}$$

being:

$$\bar{\boldsymbol{x}} = \begin{bmatrix} \hat{\alpha} \\ \hat{\beta} \end{bmatrix} \tag{129}$$

and

$$\bar{\boldsymbol{C}}_\omega = \begin{bmatrix} \frac{1}{2\hat{\omega}_{n,1}} & \frac{\hat{\omega}_{n,1}}{2} \\ \frac{1}{2\hat{\omega}_{n,2}} & \frac{\hat{\omega}_{n,2}}{2} \\ \vdots & \vdots \\ \frac{1}{2\hat{\omega}_{n,\hat{n}_z}} & \frac{\hat{\omega}_{n,\hat{n}_z}}{2} \end{bmatrix}, \quad \bar{\boldsymbol{d}}_\xi = \begin{bmatrix} \hat{\xi}_1 \\ \hat{\xi}_2 \\ \vdots \\ \hat{\xi}_{\hat{n}_z} \end{bmatrix} \tag{130}$$

where $\bar{\boldsymbol{x}}$ is the unknown vector of dimensions 2×1 containing the desired proportional coefficients $\hat{\alpha}$ and $\hat{\beta}$, $\bar{\boldsymbol{C}}_\omega$ is a coefficient matrix having dimensions $\hat{n}_z \times 2$ constructed using the identified natural angular frequencies $\hat{\omega}_{n,i},\ i = 1, 2, \ldots, \hat{n}_z$, and $\bar{\boldsymbol{d}}_\xi$ is a coefficient vector having dimensions $\hat{n}_z \times 1$ containing the identified damping ratios $\hat{\xi}_i,\ i = 1, 2, \ldots, \hat{n}_z$ of the mechanical system. In the PDC method, $\bar{\boldsymbol{C}}_\omega^+$ represents the Moore-Penrose pseudoinverse matrix of the coefficient $\bar{\boldsymbol{C}}_\omega$ matrix. Once the proportional coefficients $\hat{\alpha}$ and $\hat{\beta}$ are determined through the implementation of the PDC method, one can readily determine an improved estimation of the damping matrix as follows:

$$\hat{\boldsymbol{R}}^* = \hat{\alpha}\hat{\boldsymbol{M}} + \hat{\beta}\hat{\boldsymbol{K}} \tag{131}$$

where the matrix $\hat{\boldsymbol{R}}^*$ of dimensions $\hat{n}_z \times \hat{n}_z$ represents the improved estimation of the damping matrix identified using the PDC method. Compared with the originally identified damping matrix denoted with $\hat{\boldsymbol{R}}$, calculated using the MKR method, the improved identified damping matrix denoted with $\hat{\boldsymbol{R}}^*$, determined through the PDC method, is more consistent with the physical properties of the mechanical system under study.

4. Summary, Conclusions, and Future Work

The main goal of this work, which represents the first part of a two-part investigation, is to perform a systematic computational and experimental analysis of the principal data-driven identification procedures based on the Observer/Kalman Filter Identification Methods (OKID) and the Numerical Algorithms for Subspace State-Space System Identification (N4SID). More specifically, all the system identification computational algorithms analyzed in this two-part research paper are suitable to perform the experimental modal analysis of dynamical systems considering input-output measurements. To this end, this first paper provides a description of the fundamental analytical methods and computational algorithms employed in this two-part research study.

In this two-part research work, the applied system identification methods for obtaining first-order state-space mathematical models of mechanical systems are analyzed. To this end, the principal data-driven identification procedures based on the Observer/Kalman Filter Identification Methods (OKID) and the Numerical Algorithms for Subspace State-Space System Identification (N4SID) are considered. Subsequently, a numerical method for constructing a second-order configuration-space mathematical model from an identified first-order state-space mathematical model is studied. For this purpose, an algorithm for the identification of the Mass, Stiffness, and Damping (MKR) matrices of a mechanical system is analyzed in this investigation. Finally, the problem of improving the estimation of the damping coefficients of a given mechanical model is addressed and solved in this study by using a method for the identification of the Proportional Damping Coefficients (PDC). While the first paper of this two-part research work focuses on the analytical methods and computational algorithms of interest for this investigation, the second paper of this two-part research work deals with the presentation of the results arising from the numerical analysis and the experimental testing applied to the benchmark system and the case study considered in the paper.

As discussed in the paper, the system identification numerical techniques whose performance is studied in this research work are the OKID method and the N4SID method. In particular, the family of OKID methods analyzed in the present work is based on the Eigensystem Realization Algorithm (ERA) and the Eigensystem Realization Algorithm with Data Correlation (ERA/DC). On the other hand, the family of N4SID algorithms investigated in this research paper is based on the Canonical Variable Algorithm (CVA), the Multivariable Output-Error State Space approach (MOESP), and the Subspace System identification method that uses an AutoRegressive eXogenous model estimation-based algorithm (ARX) to compute the weighting (SSARX). The basic version of the OKID method mentioned before was implemented by the authors using a procedural approach developed in the MATLAB simulation environment, while the set of N4SID algorithms is currently available in the MATLAB System Identification Toolbox. Both the OKID method and the N4SID algorithm allow for creating a linear estimation of the first-order state-space dynamical model of the mechanical system of interest.

The estimated dynamical models are useful for realizing the experimental modal analysis as well as for control applications. In particular, the natural frequencies, the damping ratios, and the mode shapes can be effectively extracted from the identified state matrix obtained for a given mechanical system. Furthermore, two additional identification methodologies are tested in this investigation. The first technique is a method for constructing a linear estimation of the second-order configuration-space dynamical model of the mechanical system of interest starting from the identified state-space model. In this manuscript, this approach is referred to as the MKR method since it allows for computing the mass, stiffness, and damping matrices of a given mechanical system. The MKR method is, therefore, applicable to the numerical results obtained from the implementation of both the families of the OKID methods and of the N4SID algorithms. The second additional methodology considered in this paper is a technique that allows for improving the estimation of the Proportional Damping Coefficients used in the linear approximation of the damping matrix and is referred to as the PDC method. The PDC method represents a useful mathematical tool for obtaining an improved approximation of the system damping matrix, which is difficult to estimate in practical engineering applications.

There are several paths that could be followed in future work. For instance, the alternative identification procedure employed in this work for estimating the proportional damping matrix turned out to be more reliable when the damping is very small and, therefore, when the hypothesis of proportional damping is adherent to reality. However, one should be able to identify the dissipative effects of a structural system also in cases in which they are more appreciable. Another important topic that should be studied in future investigations is, therefore, the estimation of the damping coefficients. Furthermore, it would be interesting to perform a systematic comparative analysis of the system identification techniques mentioned before implemented in conjunction with the MKR method and the PDC technique considered in this work. On the other hand, the performance of several iterative identification procedures available in the literature that minimize the prediction errors to obtain maximum-likelihood values should be also analyzed in the case of real measurement data arising from experimental acquisitions. In general, the final goal of future developments related to this research work will be to exploit the identified dynamical models to design active and passive control systems that reduce the mechanical vibrations induced by external disturbances. Because of space limitations, the analysis of these challenging issues is outside of the scope of the present study and will be investigated in future research works.

Author Contributions

This research paper was principally devised and developed by the first author (Carmine Maria Pappalardo). Great support in the development of the paper was provided by the second author (Filippo Califano) and by the third author (Sefika Ipek Lok). The detailed review carried out by the fourth author (Domenico Guida) considerably improved the quality of the work. The manuscript was written with the contribution of all authors. All authors discussed the results, reviewed the methodology, and approved the final version of the manuscript.

Acknowledgments

Not applicable.

Conflict of Interest

The authors declared no potential conflicts of interest with respect to the research, authorship, and publication of this article.

Funding

The authors received no financial support for the research, authorship, and publication of this article.

Data Availability Statements

The datasets generated and/or analyzed during the current study are available from the corresponding author on reasonable request.

References

[1] Juang, J.N., *Applied system identification*, Prentice-Hall, Inc., 1994.
[2] Katamaya, T., *Subspace Methods for System Identification*, Springer-Verlag, London, 2005.
[3] Van Overschee, P., De Moor, B., *Subspace identification for linear systems: Theory—Implementation—Applications*, Springer Science & Business Media, 2012.
[4] Nelles, O., *Nonlinear system identification: from classical approaches to neural networks, fuzzy models, and gaussian processes*, Springer Nature, 2020.
[5] Moor, B.D., Overschee, P.V., Favoreel, W., Algorithms for subspace state-space system identification: an overview, *Applied and computational control, signals, and circuits*, 1999, 247–311.
[6] Tangirala, A.K., *Principles of system identification: theory and practice*, Crc Press, 2018.
[7] Reynders, E., System identification methods for (operational) modal analysis: review and comparison, *Archives of Computational Methods in Engineering*, 2012, 19(1), 51–124.
[8] Juang, J.N., Phan, M.Q., *Identification and control of mechanical systems*, Cambridge University Press, Cambridge, 2001.
[9] Pappalardo, C.M., Vece, A., Galdi, D., Guida, D., Developing a reciprocating mechanism for the emergency implementation of a mechanical pulmonary ventilator using an integrated cad-mbd procedure, *FME Transactions*, 2022, 50(2), 238–247.
[10] Serban, R., Freeman, J., Identification and identifiability of unknown parameters in multibody dynamic systems, *Multibody System Dynamics*, 2001, 5(4), 335–350.
[11] Cammarata, A., Lacagnina, M., Sinatra, R., Closed-form solutions for the inverse kinematics of the agile eye with constraint errors on the revolute joint axes, *2016 IEEE/RSJ International Conference on Intelligent Robots and Systems (IROS)*, IEEE, 317–322.
[12] Cammarata, A., Sinatra, R., Maddìo, P.D., Interface reduction in flexible multibody systems using the floating frame of reference formulation, *Journal of Sound and Vibration*, 2022, 523, 116720.
[13] Peng, T., Nogal, M., Casas, J., Lozano-Galant, J.A., Turmo, J., Constrained observability techniques for structural system identification using modal analysis, *Journal of Sound and Vibration*, 2020, 479, 115368.
[14] Jin, M., Brake, M.R., Song, H., Comparison of nonlinear system identification methods for free decay measurements with application to jointed structures, *Journal of Sound and Vibration*, 2019, 453, 268–293.
[15] Chen, J., Zhou, J., Gong, D., Sun, W., Sun, Y., You, T., Ji, Y., Identification of excitation force for under-chassis equipment of railway vehicles in frequency domain, *Journal of Vibration Engineering & Technologies*, 2021, 9(4), 701–714.

[16] Pappalardo, C.M., Guida, D., A time-domain system identification numerical procedure for obtaining linear dynamical models of multibody mechanical systems, *Archive of Applied Mechanics*, 2018, 88(8), 1325–1347.

[17] Mercère, G., Markovsky, I., Ramos, J.A., Innovation-based subspace identification in open-and closed-loop, *2016 IEEE 55th Conference on Decision and Control (CDC)*, IEEE, 2951–2956.

[18] Valasek, J., Chen, W., Observer/kalman filter identification for online system identification of aircraft, *Journal of Guidance, Control, and Dynamics*, 2003, 26(2), 347–353.

[19] Tiano, A., Sutton, R., Lozowicki, A., Naeem, W., Observer kalman filter identification of an autonomous underwater vehicle, *Control engineering practice*, 2007, 15(6), 727–739.

[20] Heredia, G., Ollero, A., Detection of sensor faults in small helicopter uavs using observer/kalman filter identification, *Mathematical Problems in Engineering*, 2011, 2011.

[21] Yang, J.N., Lin, S., Huang, H., Zhou, L., An adaptive extended kalman filter for structural damage identification, *Structural Control and Health Monitoring: The Official Journal of the International Association for Structural Control and Monitoring and of the European Association for the Control of Structures*, 2006, 13(4), 849–867.

[22] Abreu, G.L., Conceição, S.M.d., Lopes Jr, V., Brennan, M.J., Alves, M.T.S., et al., System identification and active vibration control of a flexible structure, *Journal of the Brazilian Society of Mechanical Sciences and Engineering*, 2012, 34(SPE), 386–392.

[23] Gagg F, L., Da Conceição, S., Vasques, C., De Abreu, G., Lopes, V., Brennan, M., et al., Experimental identification and control of a cantilever beam using era/okid with a lqr controller, *Journal of Control, Automation and Electrical Systems*, 2014, 25(2), 161–173.

[24] Ni, Z., Wu, S., Zhang, Y., Wu, Z., Payload parameter identification of a flexible space manipulator system via complex eigenvalue estimation, *International Journal of Aerospace Engineering*, 2020, 2020.

[25] Favoreel, W., De Moor, B., Van Overschee, P., Subspace state space system identification for industrial processes, *Journal of process control*, 2000, 10(2-3), 149–155.

[26] Douat, L.R., Queinnec, I., Garcia, G., Michelin, M., Pierrot, F., Tarbouriech, S., Identification and vibration attenuation for the parallel robot par2, *IEEE Transactions on Control Systems Technology*, 2013, 22(1), 190–200.

[27] Junior, A.C., Riul, J.A., Montenegro, P.H.M., Application of the subspace identification method using the n4sid technique for a robotic manipulator, *IEEE Latin America Transactions*, 2016, 14(4), 1588–1593.

[28] Costa, A.G., Maldonado, J.L.B., Romero, F.A., Sanmartín, J.C., Valarezo, M., Castillo, H., N4sid method applied to obtain a discrete-time linear state space system as a mathematical model of a jaw crusher prototype, *2017 CHILEAN Conference on Electrical, Electronics Engineering, Information and Communication Technologies (CHILECON)*, IEEE, 1–6.

[29] Lus, H., Betti, R., Yu, J., De Angelis, M., Investigation of a system identification methodology in the context of the asce benchmark problem, *Journal of Engineering Mechanics*, 2004, 130(1), 71–84.

[30] De Angelis, M., Lus, H., Betti, R., Longman, R.W., Extracting physical parameters of mechanical models from identified state-space representations, *J. Appl. Mech.*, 2002, 69(5), 617–625.

[31] Lus, H., De Angelis, M., Betti, R., Longman, R.W., Constructing second-order models of mechanical systems from identified state space realizations. part i: theoretical discussions, *Journal of Engineering Mechanics*, 2003, 129(5), 477–488.

[32] Lus, H., De Angelis, M., Betti, R., Longman, R.W., Constructing second-order models of mechanical systems from identified state space realizations. part ii: Numerical investigations, *Journal of engineering mechanics*, 2003, 129(5), 489–501.

[33] Rabah, S., Coppier, H., Chadli, M., Azimi, S., Rocher, V., Escalon, D., Zoghlami, N., Naceur, M., Multi-variable industrial processes identification: Case of bubbling fluidized bed sewage sludge incinerator, *2016 24th Mediterranean Conference on Control and Automation (MED)*, IEEE, 803–808.

[34] Anandakumar, P., Jacob, J., Structural and crack parameter identification on structures using observer kalman filter identification/eigen system realization algorithm, 2021.

[35] Piramoon, S., Ayoubi, M.A., An eigensystem realization algorithm for modal parameter identification of a vertical-shaft high-speed centrifugal machine, *ASME International Mechanical Engineering Congress and Exposition*, vol. 84546, American Society of Mechanical Engineers, V07AT07A032.

[36] Iyer, V.V., Johnson, E.N., Singla, P., Observer controller identification of a medium-weight co-axial octocopter, *AIAA SCITECH 2022 Forum*, 1083.

[37] Huang, Z., Xi, F., Huang, T., Dai, J.S., Sinatra, R., Lower-mobility parallel robots: theory and applications, 2010.

[38] Phan, M., Horta, L.G., Juang, J.N., Longman, R.W., Improvement of observer/kalman filter identification (okid) by residual whitening, 1995.

[39] Guida, D., Nilvetti, F., Pappalardo, C.M., Parameter identification of a two degrees of freedom mechanical system, *International Journal of Mechanics*, 2009, 3(2), 23–30.

[40] Sampaio Silveira Júnior, J., Marques Costa, E.B., Fuzzy modelling methodologies based on okid/era algorithm applied to quadrotor aerial robots, *Intelligent Systems: Theory, Research and Innovation in Applications*, Springer, 2020, 295–317.

[41] Subramanian, S., Chidhambaram, G.B., Dhandapani, S., Modeling and validation of a four-tank system for level control process using black box and white box model approaches, *IEEJ Transactions on Electrical and Electronic Engineering*, 2021, 16(2), 282–294.

[42] Manrique-Escobar, C.A., Pappalardo, C.M., Guida, D., On the analytical and computational methodologies for modelling two-wheeled vehicles within the multibody dynamics framework: A systematic literature review, *Journal of Applied and Computational Mechanics*, 2021.

[43] Pappalardo, C.M., Guida, D., System identification and experimental modal analysis of a frame structure., *Engineering Letters*, 2018, 26(1).

[44] Pappalardo, C.M., Guida, D., Development of a new inertial-based vibration absorber for the active vibration control of flexible structures., *Engineering Letters*, 2018, 26(3).

[45] Borjas, S., Garcia, C., Subspace identification for industrial processes, *TEMA (São Carlos)*, 2011, 12, 183–194.

[46] Juricek, B.C., Seborg, D.E., Larimore, W.E., Identification of the tennessee eastman challenge process with subspace methods, *Control Engineering Practice*, 2001, 9(12), 1337–1351.

[47] Mola, M., Khanesar, M.A., Teshnehlab, M., Subspace identification of dynamical neurofuzzy system using lolimot, *2010 IEEE International Conference on Systems, Man and Cybernetics*, IEEE, 366–372.

[48] Brunton, S.L., Dawson, S.T., Rowley, C.W., State-space model identification and feedback control of unsteady aerodynamic forces, *Journal of Fluids and Structures*, 2014, 50, 253–270.

[49] Tronci, E., Pietrosanti, D., Cordisco, G., De Angelis, M., Vibration analysis of the civic tower in rieti, *Procedia engineering*, 2017, 199, 2268–2273.

[50] Borjas, S.D.M., Garcia, C., Identificação determinística por subespaços, *TEMA (São Carlos)*, 2012, 13, 207–218.

[51] Mercère, G., Bako, L., Parameterization and identification of multivariable state-space systems: A canonical approach, *Automatica*, 2011, 47(8), 1547–1555.

[52] Deistler, M., Peternell, K., Scherrer, W., Consistency and relative efficiency of subspace methods, *Automatica*, 1995, 31(12), 1865–1875.

[53] Peternell, K., Scherrer, W., Deistler, M., Statistical analysis of novel subspace identification methods, *Signal Processing*, 1996, 52(2), 161–177.

[54] Jamaludin, I., Wahab, N., Khalid, N., Sahlan, S., Ibrahim, Z., Rahmat, M.F., N4sid and moesp subspace identification methods, *2013 IEEE 9th International Colloquium on Signal Processing and its Applications*, IEEE, 140–145.

[55] Flint, T.W., Vaccaro, R.J., Performance analysis of n4sid state-space system identification, *Proceedings of the 1998 American Control Conference. ACC (IEEE Cat. No. 98CH36207)*, vol. 5, IEEE, 2766–2767.

[56] Simay, V., Verhaegenz, M., Comparative study between three subspace identification algorithms.

[57] Heredia, G., Ollero, A., Sensor fault detection in small autonomous helicopters using observer/kalman filter identification, *2009 IEEE International Conference on Mechatronics*, IEEE, 1–6.

[58] Chang, M., Pakzad, S.N., Observer kalman filter identification for output-only systems using interactive structural modal identification toolsuite, *Journal of Bridge Engineering*, 2014, 19(5), 04014002.

[59] Qin, S.J., An overview of subspace identification, *Computers & chemical engineering*, 2006, 30(10-12), 1502–1513.

[60] Dong, X.J., Meng, G., Peng, J.C., Vibration control of piezoelectric smart structures based on system identification technique: Numerical simulation and experimental study, *Journal of sound and vibration*, 2006, 297(3-5), 680–693.

[61] Wang, J.S., Hsu, Y.L., Dynamic nonlinear system identification using a wiener-type recurrent network with okid algorithm., *Journal of Information Science & Engineering*, 2008, 24(3).

[62] Bauer, D., Jansson, M., Analysis of the asymptotic properties of the moesp type of subspace algorithms, *Automatica*, 2000, 36(4), 497–509.

[63] Cammarata, A., Sinatra, R., Rigano, A., Lombardo, M., Maddio, P.D., Design of a large deployable reflector opening system, *Machines*, 2020, 8(1), 7.

[64] Maddio, P.D., Salvini, P., Sinatra, R., Cammarata, A., Optimization of the efficiency of large deployable reflectors by measuring the error around the feed, *Acta Astronautica*, 2022, 199, 206–223.
[65] Aktas, B., Cecen, F., Ozturk, H., Navdar, M.B., Ozturk, I.S., Comparison of prestressed concrete railway sleepers and new lcr concrete sleepers with experimental modal analysis, *Engineering Failure Analysis*, 2022, 131, 105821.
[66] Wang, Y., Egner, F.S., Willems, T., Kirchner, M., Desmet, W., Camera-based experimental modal analysis with impact excitation: Reaching high frequencies thanks to one accelerometer and random sampling in time, *Mechanical Systems and Signal Processing*, 2022, 170, 108879.
[67] Koyuncu, A., Karaauacli, T., Sahin, M., Ozguven, H., Experimental modal analysis of nonlinear amplified piezoelectric actuators by using response-controlled stepped-sine testing, *Experimental Mechanics*, 2022, 1–16.
[68] Song, C., Fan, W., Dong, J., Zhao, Y., Lu, L., Mi, P., Xu, Y., Hou, L., Liu, T., Modal analysis of 3d multi-axial hybrid composite with experimental and numerical methods, *Applied Composite Materials*, 2022, 29(1), 27–41.
[69] Berninger, T.F., Seiwald, P., Sygulla, F., Rixen, D.J., Evaluating the mechanical redesign of a biped walking robot using experimental modal analysis, *Topics in Modal Analysis & Testing, Volume 8*, Springer, 2022, 45–52.
[70] Wang, S., Jin, S., Bai, D., Fan, Y., Shi, H., Fernandez, C., A critical review of improved deep learning methods for the remaining useful life prediction of lithium-ion batteries, *Energy Reports*, 2021, 7, 5562–5574.
[71] Wang, S., Takyi-Aninakwa, P., Jin, S., Yu, C., Fernandez, C., Stroe, D.I., An improved feedforward-long short-term memory modeling method for the whole-life-cycle state of charge prediction of lithium-ion batteries considering current-voltage-temperature variation, *Energy*, 2022, 124224.
[72] Wang, Y., Li, M., Chen, Z., Experimental study of fractional-order models for lithium-ion battery and ultra-capacitor: Modeling, system identification, and validation, *Applied Energy*, 2020, 278, 115736.
[73] Peng, N., Zhang, S., Guo, X., Zhang, X., Online parameters identification and state of charge estimation for lithium-ion batteries using improved adaptive dual unscented kalman filter, *International Journal of Energy Research*, 2021, 45(1), 975–990.
[74] Ren, B., Xie, C., Sun, X., Zhang, Q., Yan, D., Parameter identification of a lithium-ion battery based on the improved recursive least square algorithm, *IET Power Electronics*, 2020, 13(12), 2531–2537.
[75] Ljung, L., et al., Theory for the user, *System Identification*, 1987.
[76] Ewins, D.J., *Modal testing: theory, practice and application*, John Wiley & Sons, 2009.
[77] Gawronski, W.K., *Dynamics and control of structures: A modal approach*, Springer Science & Business Media, 2004.
[78] Juang, J.N., Phan, M.Q., *Identification and control of mechanical systems*, Cambridge University Press, 2001.
[79] HO, B., Kálmán, R.E., Effective construction of linear state-variable models from input/output functions, *at-Automatisierungstechnik*, 1966, 14(1-12), 545–548.
[80] Juang, J.N., Cooper, J.E., Wright, J., An eigensystem realisation algorithm using data correlations (era/dc) for modal parameter identification, *Control-theory and advanced technology*, 1988, 4(1), 5–14.

ORCID iD

Carmine Maria Pappalardo https://orcid.org/0000-0003-3763-7104
Filippo Califano https://orcid.org/0000-0002-3481-2758
Sefika Ipek Lok https://orcid.org/0000-0002-5344-5615
Domenico Guida https://orcid.org/0000-0002-2870-9199

How to cite this article: Carmine Maria Pappalardo, Filippo Califano, Sefika Ipek Lok, Domenico Guida. A Systematic Computational and Experimental Study of the Principal Data-Driven Identification Procedures. Part I: Analytical Methods and Computational Algorithms, J. Appl. Comput. Mech., 9(2), 2023, 529-549. https://doi.org/10.22055/jacm.2022.41537.3770